



Review

Three-dimensional polymer networks for solid-state electrochemical energy storage

Zhong Xu^{a,1}, Xiang Chu^{a,1}, Yihan Wang^a, Haitao Zhang^{a,*}, Weiqing Yang^{a,b,*}

^a Key Laboratory of Advanced Technologies of Materials (Ministry of Education), School of Material Science and Engineering, Southwest Jiaotong University, Chengdu 610031, PR China

^b State Key Laboratory of Traction Power, Southwest Jiaotong University, Chengdu 610031, PR China

HIGHLIGHTS

- 3D polymer applied in solid-state energy storage has been comprehensively reviewed.
- The synthesis strategy and advantages of 3D polymer for SSCs and SSLIBs are presented.
- The modification motivation and properties of 3D polymer are stated very carefully.
- The challenges of future development for 3D polymer is also proposed in this review.

ARTICLE INFO

Keywords:

Three-dimensional polymer networks
Solid-state electrochemical energy storage
Lithium-ion battery
Supercapacitors
Electrodes
Electrolytes

ABSTRACT

Solid-state electrochemical energy storage devices (i.e. supercapacitors and lithium-ion batteries) have attracted tremendous attention because they are widely considered as the promising next-generation energy/power technology to overcome the current issues of low energy density and insecure safety in conventional liquid devices. The last decade we witnessed notable performance improvement on electrochemical energy storage through advances in understanding and design of advanced nanostructured materials. One could argue that inorganic materials have played a central, starring role for the assembly of various electrochemical energy storage systems. However, energy storage systems fabricated from organic polymer networks have just emerged as a new prospect. 3D polymer is a category of pure polymer or composites featuring three-dimensional frameworks structure, which could be potentially used in solid-state electrochemical energy storage due to its high electron conductivity or ionic conductivity. Here we summarize the main research advances on the attractive use of 3D polymer networks for the fabrication of electrodes and electrolytes in either solid-state supercapacitors or lithium-ion batteries. Besides, challenges of future development for 3D polymer networks have also been outlined.

1. Introduction

The rapid growth of global population and economic prosperity is now leading to significantly increasing demand for energy. However, conventional energy resources such as petroleum, coal and natural gas with limited reserves can't support the long-term prosperity of human society [1,2]. In this regard, researchers are appealing to technologies for harvesting renewable energies including solar energy, wind and blue energy [3,4]. To convert the intermittent and randomly occurred renewable energy into continuous and reliable power supply, it is of

great necessity to develop high efficient, stable and environmentally friendly energy storage devices. Additionally, flexible and wearable electronics such as smart watch and foldable cell phone have become hotspot consumer products in modern society, which correspondingly stimulates the proliferation of solid-state energy storage devices [5,6]. Solid-state supercapacitors (SSCs) and all solid-state lithium-ion batteries (ASSLIBs) are two typical starring members with both remarkable electrochemical performance and high security in the big family of electrochemical energy storage devices (inset of Fig. 1) [7,8]. SSCs storing electrochemical energy through either fast physical electrostatic

* Corresponding authors at: Key Laboratory of Advanced Technologies of Materials (Ministry of Education), School of Material Science and Engineering, Southwest Jiaotong University, Chengdu 610031, PR China (W. Yang).

E-mail addresses: haitaozhang@swjtu.edu.cn (H. Zhang), wqyang@swjtu.edu.cn (W. Yang).

¹ Zhong Xu and Xiang Chu contributed equally to this work.

<https://doi.org/10.1016/j.cej.2019.123548>

Received 15 May 2019; Received in revised form 12 November 2019; Accepted 18 November 2019

Available online 19 November 2019

1385-8947/ © 2019 Elsevier B.V. All rights reserved.

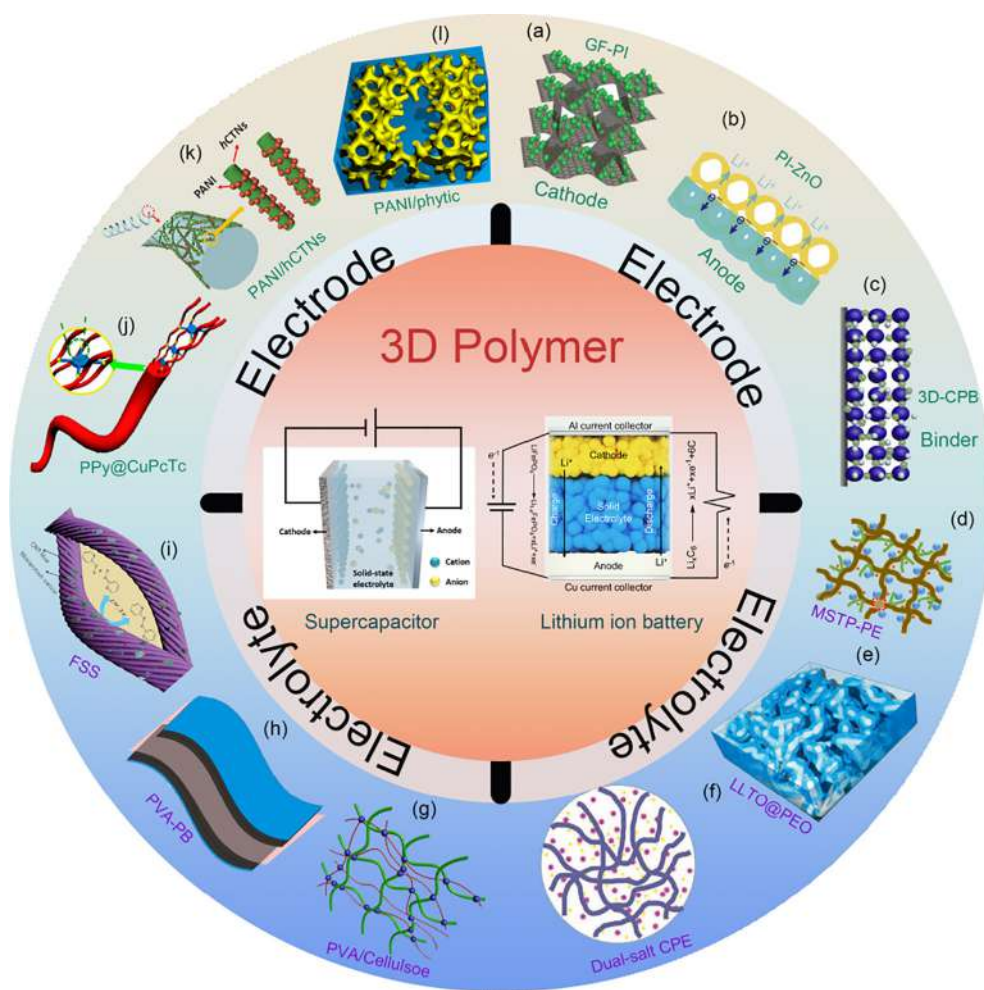


Fig. 1. Different applications of 3D polymers in solid-state supercapacitors and lithium-ion batteries. (a) GF-PI [16] Copyright 2017, Royal Society of Chemistry, (b) 3D PI-ZnO [17] Copyright 2016, Nature Publishing Group, (c) 3D CPB [18] Copyright 2018, Elsevier Science Inc, (d) MSTP-PE [19] Copyright 2017, Elsevier Science Inc, (e) LLTO@PEO [20] Copyright 2017, Wiley, (f) dual-salt 3D-CPE [21] Copyright 2018, Wiley, (g) PVA/cellulose [22] Copyright 2019, Springer, (h) PVA-PB [23] Copyright 2012, Elsevier Science Inc, (i) FSS [24] Copyright 2015, Royal Society of Chemistry, (j) PPy@CuPcTs [25] Copyright 2015, American Chemical Society (k) PANI/hCNTs [26] Copyright 2019, Elsevier Science Inc, (l) PANI/phytic [27] Copyright 2012, PNAS.

adsorption process (Electrical double layer capacitor, EDLC) or rapid surface redox reaction (Pseudo-capacitor) feature rapid charge/discharge dynamics, high power density and exceptional long cycling life [9–12]. In contrast, ASSLIBs possess much higher energy density with high working voltage (> 3.8 V) and thus are attracted great attention. Moreover, ASSLIBs held the significant advantage of excellent safety (No explosion and leakage risk) that is one of the greatest issues in conventional liquid devices. Similarly, ASSLIBs consist of cathode, solid-state electrolyte, anode and current collectors. The lithium ion can insert/extract in electrode and transport via solid electrolyte according to the different mechanism such as ion transition theory, vacancy transport theory and so on [13]. Unlike the conventional liquid-based lithium ion batteries, the ASSLIBs replace the liquid organic electrolyte with solid-state electrolyte which can extremely enhance the safety as well as the energy density with lithium anode.

To date, inorganic materials such as activated carbon, graphite anodes and lithium transition metal oxides have been successfully applied in commercialized supercapacitors and lithium ion batteries and is now playing indispensable role in our daily life [14]. However, the electrochemical performance of these devices such as energy density, power density and cycling stability is still far from satisfying the growing demand [15]. In this regard, we have seen increasing interest in the rational design and synthesis of electrode and electrolyte materials with unique nanostructures. Three-dimensional (3D) polymers, an emerging class of organic materials consisting of pure polymers or polymer composites, possessing interconnected 3D networks and highly continuous porous structure, could be utilized in both electrodes and electrolytes of SSCs and ASSLIBs. When 3D polymers are utilized as electrode materials, they can naturally form conductive scaffolds for

electrons and unblocked pathways for electrolyte penetration, an efficient electrode/electrolyte interface can thus be obtained. When 3D polymers are utilized as electrolyte materials, they play the dual role of both electrolytic salt host matrix and separator. In addition, the copious pore volume of 3D polymers will facilitate the ion/mass transfer in electrolyte, which will lead to efficient electrochemical process and rapid electrochemical response. Here, we review recent advances in 3D polymer based solid-state electrochemical energy storage devices (mainly in SSCs and ASSLIBs), including the 3D electrode (cathode, anode and binder) and electrolyte (as shown in Fig. 1). We mainly focus on the fabrication strategies of constructing 3D nanostructures and corresponding electrochemical performance. Advantages and disadvantages of each strategy is elaborately analyzed and remaining challenges are clarified. Moreover, perspectives and opportunities of 3D polymers will be discussed as well.

2. 3D polymers for solid-state supercapacitors

Solid-state supercapacitors (SSCs) recently emerged as a promising energy storage device featuring exceptionally long cycle life, large power density, high security and reliability along with environmental benignity [7,8]. SSCs commonly consist of current collector, electrochemical active electrodes, solid-state electrolyte and encapsulating layers, among which electrodes and solid-state electrolytes play crucial role in determining electrochemical performance of devices. In contrast with conventional liquid supercapacitors, SSCs perfectly avoid the electrolyte leakage in combination with larger potential window. Additionally, the separator membrane can also be avoided since the solid-state electrolyte can play dual role of ion transfer and electron isolation.

One could argue that inorganic hybrid materials have played a central, starring role for the assembly of SSCs. However, organic materials such as 3D polymer networks are playing significantly important role in the fabrication of advanced SSCs. To date, various 3D polymer materials have been reported for the fabrication of both electrodes and electrolytes for SSCs. Therefore, in this section, we will discuss recent advances in 3D polymer-based SSC electrodes, including 3D polymer derivatives especially conducting polymer hydrogels and 3D conducting polymer/carbonaceous materials composites. Besides, different types of gel polymer electrolytes are introduced in the following part in which 3D polymer networks basically serve as the host matrix.

2.1. 3D polymer electrodes for SSCs

Electrode materials of SSCs play an unambiguously crucial role in determining the electrochemical performance of device due to their either large accessible surface area (electrochemical double layer capacitors) or intrinsic fast surface redox reactions (pseudo-capacitors) [28]. Recently, a remarkable improvement in performance of SSCs have been achieved through advances in electrochemical active electrodes such as carbonaceous materials [29–31], transition metal oxides [32,33] and conducting polymers (CPs) [34,35]. Generally, the vast majority of existing polymers can't be applied in the fabrication of SSCs electrodes because they are insulating and electrochemically inactive. Only a few kinds of CPs such as polyaniline (PANI), polypyrrole (PPy), poly(3,4-ethylenedioxythiophene) (PEDOT) and their derivatives can be used as SSCs electrodes because rapid redox reaction happened on the surface of these polymers and electrochemical energy can thus be stored/released. According to previously reported literatures, CPs such as PANI store energy through redox transition between leucoemeraldine (insulating) and protonated emeraldine (conducting), the transition between p-benzoquinone and hydroquinone, and the transition between emeraldine and the pernigraniline. These redox peaks embedded in a high background current indicate a pseudocapacitive performance of PANI [9]. Moreover, CPs polymeric chains can be reversibly doped/de-doped by electrolytic ions, thus ions can be temporarily stored by CPs. Compared with bulk CPs, 3D CPs inherit the above-mentioned merits while possess hierarchical 3D architectures simultaneously, which consequently guarantee more efficient contact between electrode and electrolyte as well as unblocked transport channel of solvated ions, and hence leading to promising electrochemical properties. Generally, there are two typical strategies towards construction of 3D CP electrodes: (i) Building 3D conducting polymer hydrogels (CPHs) for SSCs electrodes. CPHs are a type of monolithic scaffold superstructures comprising CPs nanoparticles or nanosheets, not only inherit remarkable properties of CPs such as relatively high conductivity, considerable softness, unique conjugated chain structure and intrinsic large pseudo-capacitance, but also offer 3D interconnected networks with unique properties of large surface area, outstanding mechanical durability, and high ion transmission efficiency. Due to the fact that the solid phase of CPHs is completely surrounded by large amounts of liquid phase, the electrochemical materials can be fully utilized. Further, extra surface area and molecular contact of electrode materials and electrolyte can also be achieved benefiting from the swelling behavior of polymer with water and ions, which leads to the efficient electrochemical process of supercapacitors. (ii) Inclusion of CPs into scaffolds possessing stable 3D architectures. Since it is still a big challenge to spontaneously construct pure CPs into advanced 3D hierarchical structures because of rigid macromolecular chains and poor processability. CPs can be rationally incorporated into existing 3D networks such as carbonaceous frameworks to form 3D hierarchical structures.

2.1.1. 3D CPHs for SSCs

3D CPHs appeared as an emerging class of derivatives of CPs, which advantageously synergize the features of hydrogels and organic

conductors. 3D CPHs have gain ground in a variety of applications such as sensors [36,37], catalysis [38], drug delivery [39,40] and energy storage [41,42]. CPHs are generally cross-linked networks containing a significant amount of water serves as the medium. The hydrophilic nature and interconnected porous structure of CPHs give rise to easy penetration of electrolyte and molecular level contact between the electrode materials and electrolyte, resulting in an extremely high effective surface area [43]. Besides, the inherent soft nature of hydrogel materials endows the electrode superior flexibility, which benefits to gain high performance devices with promising flexibility. Compared with rigid electrode materials such as active carbon and transition metal oxides, CPHs can be directly used as the electrode materials through facilely integrating it onto current collector during in-situ gelation, thus we can eliminate the utilization of binder such as carboxymethyl cellulose (CMC), polyvinylidene fluoride (PVDF) and polytetrafluoroethylene (PTFE). Additionally, some recently reported CPHs could even be sprayed or screen-printed into pre-designed micro-patterns, which makes them promising candidate for massive fabrication of all-printed electrochemical devices [27,44].

2.1.1.1. 3D CPHs with non-conductive frameworks. To construct a 3D CPHs system, a conventional method is synthesizing or polymerizing conductive polymer monomer within an existing nanostructured hydrogel matrix that basically serve as templates and frameworks (As shown in Fig. 2a). In this context, Wang et al. [45] designed an all-in-one flexible supercapacitor through integrating two PANI layers with 40 μm thickness into chemically crosslinked PVA/ H_2SO_4 hydrogel film. This device possesses a distinct three-layer structure, in which the top and bottom layer are electrochemical active PANI while the middle layer is glutaraldehyde (GA) gelled PVA/ H_2SO_4 hydrogel film. In this typical sandwiched configuration, GA gelled PVA/ H_2SO_4 hydrogel is employed as both electrolyte and 3D template of PANI. CPHs layer can be successfully incorporated onto PVA/ H_2SO_4 hydrogel matrix through immersing it into aniline dilute solution. Consequently, this hydrogel exhibits high break stretching of 300% with a fracture stress of 0.35 MPa and the resultant flexible SSCs deliver a high areal capacitance of 488 mF cm^{-2} at the current density of 0.2 mA cm^{-2} . To enhance the strength and robustness of CPHs, covalent bond

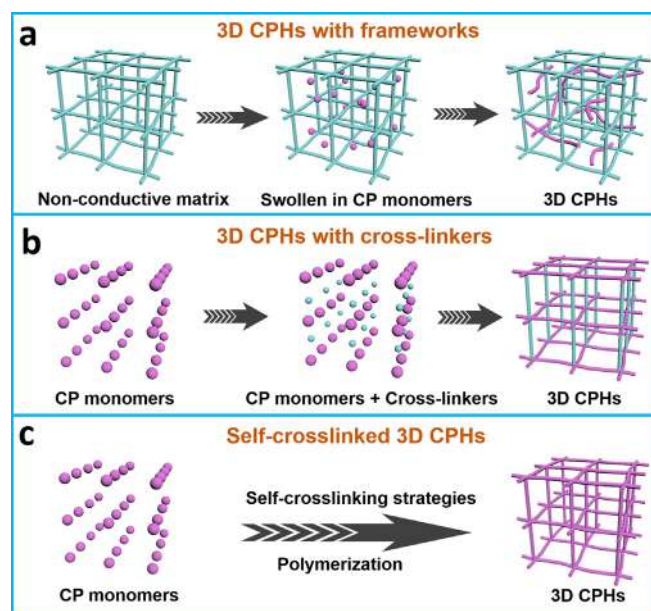


Fig. 2. Typical synthetic methods toward 3D CPHs. (a) Synthesizing CPs in existing non-conductive polymer frameworks. (b) Adding cross-linkers with multiple functional groups into CPs to build 3D CPHs. (c) Using self-crosslinking strategies towards 3D CPHs.

between CPs and hydrogel matrix is often introduced into the hybrid system. For instance, Li and co-workers [46] reported a supramolecular strategy to prepare conductive hydrogels for the fabrication of high performance SSCs, in which dynamic boronate bond is elaborately introduced in between rigid conductive PANI and soft hydrophilic PVA chains. As a result, this CPHs show enhanced robustness with a Young's modulus of 27.9 MPa and tensile strength of 5.3 MPa at 250% elongation. Flexible SSCs based on this CPHs provides a large capacitance (306 mF cm^{-2} and 153 F g^{-1}) and a high energy density of 13.6 Wh kg^{-1} . The robustness of the SSCs is demonstrated by 100% capacitance retention after 1000 mechanical folding cycles. Similarly, Zhang et al. [47] covalently incorporated PANI onto a triblock copolymer (IAOAI) containing a central poly (ethylene oxide) block and terminal poly (acrylamide) (PAAm) block with aniline moieties randomly incorporated. Morphology characterization reveals that these CPHs consist of well-ordered pores with an average size of $30 \mu\text{m}$, which could facilitate the mass transfer and the free moving of electrolyte. Enlarged SEM picture shows the CPHs scaffold is composed of numerous 50 nm nanoparticles, thus the specific surface area of hydrogel can be remarkably enhanced. Besides, these CPHs exhibit high conductivity of 0.15 S cm^{-1} as well as promising elongation of 112% with a tensile stress of 11 kPa. As a result, these CPHs demonstrate remarkable electrochemical capacitance (919 F g^{-1}) along with good cyclic stability (90% capacitance retention after 1000 cycles). Moreover, supercapacitors based on the hybrid hydrogel electrodes present a large specific capacitance (187 F g^{-1}) and considerable flexibility. In summary, this method is versatile and effective to construct CPHs networks and the mechanical performance of CPHs can be easily tuned through choosing proper hydrogel matrix. However, the specific capacitance and volumetric energy density is often limited due to the existence of non-conductive frameworks, which is generally electrochemical inactive and thus impairs electrochemical performance.

2.1.1.2. 3D CPHs with novel cross-linkers. In the above-mentioned system, a nonconductive hydrogel matrix is always employed as template or framework to build 3D hybrid CPHs, which will inevitably lead to deterioration of both electrical and electrochemical properties. In this regard, it is of great necessity to reduce the proportion of electrochemical inactive component while increase the proportion of electrochemical active component (CPs) in the CPHs system to capture high electrochemical performance. A typical method toward CPHs with high electrochemical performance is introducing cross-linker that contains multiple functional groups into CPs, which could consequently interact with CP chains and finally lead to 3D crosslinked networks (Fig. 2b). In this context, Pan et al. [27] employed phytic acid as both dopant and cross-linker for the construction of PANI based CPHs. The gelation mechanism of PANI hydrogel is illustrated in Fig. 3a. Phytic acid reacts with PANI by protonating the nitrogen groups on PANI. Since each phytic acid molecule can interact with more than one PANI chain, this crosslinking effect results in the formation of a mesh-like hydrogel network and rapid gelation of mixed solution of approximate 3 min (Fig. 3b). Notably, this PANI based CPHs exhibits a high conductivity of 0.11 S cm^{-1} at room temperature and electronic conductivity of dehydrated powder was measured to be 0.23 S cm^{-1} by a standard four-point-probe method. Morphology characterization reveals the 3D porous foam structure of CPHs with interconnected coral-like dendritic nanofibers (Fig. 3c). Such 3D interconnected PANI nanofiber structures can be more effective than wires and particles for electrochemical device applications due to large open channels of the micron-scale and nanometer-scale pores within the structure. Due to the high conductivity and hierarchical porosity, this polyaniline based CPHs demonstrate high specific capacitance (480 F g^{-1}), unprecedented rate capability, and cycling stability ($\sim 83\%$ capacitance retention after 10,000 cycles). To demonstrate the versatility of phytic acid for constructing 3D CPHs, Shi et al. [48]

reported a unique 3D porous nanostructured conductive polypyrrole (PPy) hydrogel via an interfacial polymerization method in which the polymerization is carried out at an organic/aqueous biphasic interface. The morphology and relevant mechanical and electrochemical properties of the PPy-based CPHs could be tuned by controlling the ratio of phytic acid to pyrrole monomers in the synthetic process. Consequently, the obtained SSCs shows a specific capacitance of $\sim 380 \text{ F g}^{-1}$, excellent rate capability, and high areal capacitance of $\sim 6.4 \text{ F cm}^{-2}$ at a mass loading of 20 mg cm^{-2} . Since multiple organic acids used as cross-linkers is an effective agent to construct 3D CPHs, Dou and co-workers [44] reported that amino trimethylene phosphonic acid (ATMP, a water treatment agent) can be employed as the gelator and dopant because its phosphorus groups serve as strongly acidic groups to dope PANI and render PANI CPH a significant hydrophilicity (Shown in Fig. 3d). Additionally, this PANI CPH with considerable electrochemical performance (422 F g^{-1}) can be further processed through 3D multilayer printing or screen printing into micro-patterns due to the unique synthesis method and desirable processability, which paves the way toward scalable fabrication of micro-supercapacitors.

In addition to multiple organic acids, other cross-linkers such as dopant counterion or multivalent metal ions have also been applied into the fabrication of high performance CPHs. For instance, Wang et al. [25] reported a disc-shaped liquid crystal molecular copper phthalocyanine-3,4',4'',4'''-tetrasulfonic acid tetrasodium salt (CuPcTs) cross-linked PPy CPHs with enhanced conductivity and pseudocapacitance (Fig. 3e). In this CPHs system, the CuPcTs acts as both the dopant and gelator to self-assemble the PPy into nanostructured hydrogels through electrostatic interaction and hydrogen bonding between the tetra-functional CuPcTs and PPy chain. The resultant CuPcTs-doped PPy CPHs consist of interconnected nanofibers with diameter of $\sim 60 \text{ nm}$, 3D interconnected framework can thus be constructed. Notably, PPy was just employed as a model system in this research, other typical CPs such as PANI and PEDOT were also demonstrated to be effective for the construction of 3D CPHs networks when CuPcTs was utilized as gelator. Consequently, the CuPcTs-PPy hydrogel exhibit higher electrochemical performance ($\sim 400 \text{ F g}^{-1}$ at 0.2 A g^{-1}) than pure PPy attributed to higher conductivity and unique interconnected structure. In particular, Dai et al. [49] reported that a self-strengthened PEDOT-PSS hydrogel could be formed in one step through the polymerization of EDOT in the presence of PSS with Fe^{3+} ions acting as both the oxidant and the ionic cross-linker. This PEDOT-PSS hydrogel demonstrated both high fracture stress up to 3.3 MPa with a fracture strain of 90% and high conductivity in the order of $10^{-2} \text{ S cm}^{-1}$. Compared with the first synthetic route in which non-conductive frameworks is employed, adding cross-linkers could be an efficient way to decrease to proportion of electrochemical inactive component and consequently enhance electrochemical performance. Nevertheless, in most cases the weak interactions such as hydrogen bond or electrostatic interaction between cross-linkers and polymer chains will lead to poor strength and robustness.

2.1.1.3. 3D CPHs with self-crosslinking strategies. Although adding cross-linkers into CP systems is demonstrated to be an effective way towards 3D CPHs, the cross-linkers are generally non-conductive and will consequently hamper specific capacitance and energy density of CPHs. In this regard, it is superior to develop self-crosslinked CPHs in the absence of extra cross-linkers. Guo et al. [50] reported a self-crosslinking strategy towards 3D PANI CPHs via oxidative coupling reaction with using ammonium persulfate as the oxidizing agent and aniline hydrochloric salt as the precursor in the absence of any additional cross-linkers (Fig. 2c). Due to the absence of any additional cross-linkers, this CPHs exhibit high specific capacitance of 750 F g^{-1} , which is a new record at that time. Similarly, Yao et al. [51] reported a facile method of preparing PEDOT:PSS hydrogel by thermal treatment of commercial PEDOT:PSS suspension in sulfuric acid. The resultant hydrogel exhibits high conductivity of 8.8 S cm^{-1} and highly porous structure. Additionally, this CPHs can be easily fabricated into

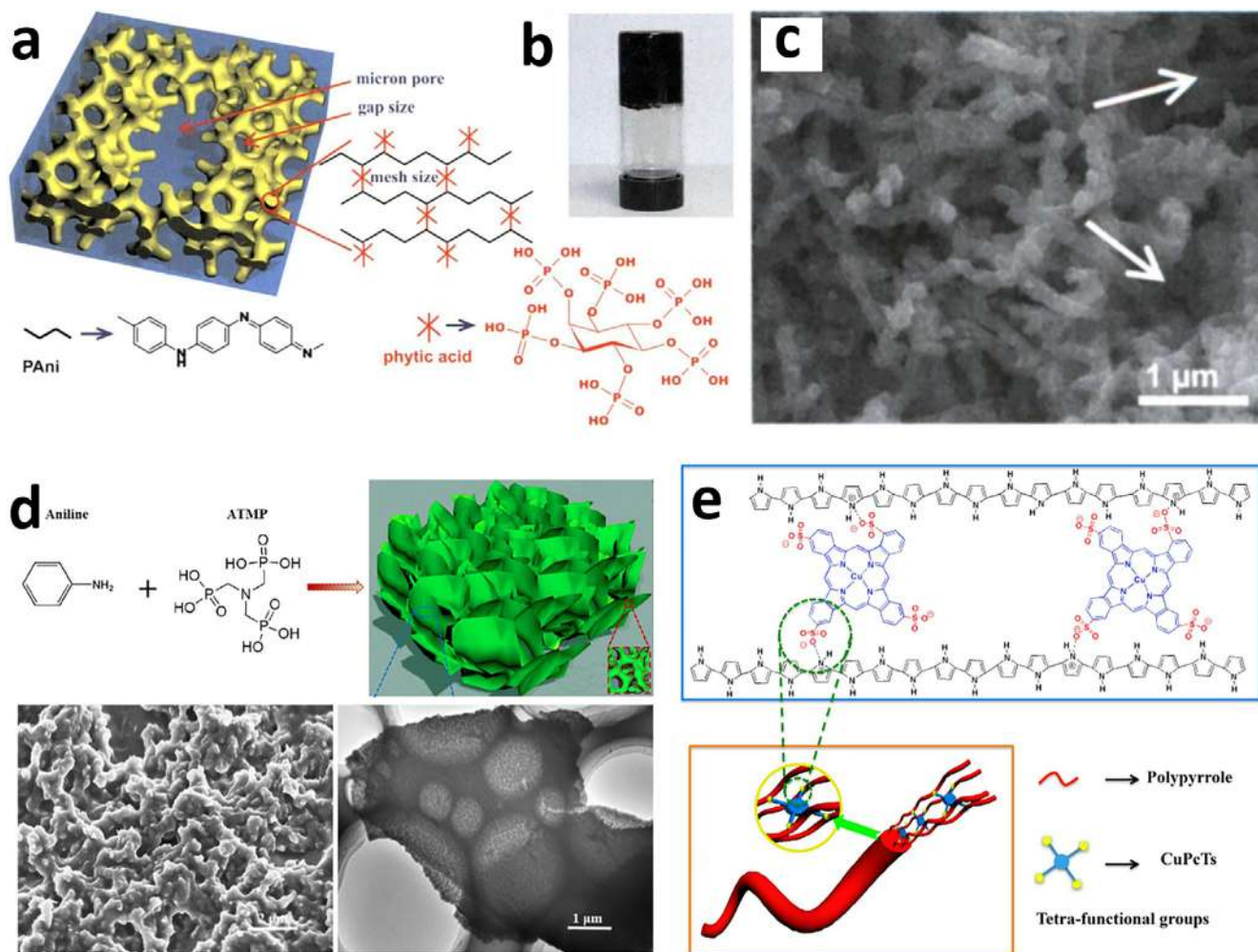


Fig. 3. (a) Schematic illustration of preparing 3D hierarchical PANI hydrogel where phytic acid plays dual role of cross-linker and dopant. (b) Digital image of PANI/phytic acid in a reversed glass vial. (c) SEM image of porous dehydrated hydrogel. Reprinted with permission [27]. Copyright 2012, PNAS. (d) Schematic illustration of preparing 3D PANI hydrogel with amino trimethylene phosphonic acid serves as cross-linker and corresponding morphology. Reprinted with permission [44]. Copyright 2016, Springer. (e) The PPy hydrogel crosslinked by disc-shaped liquid crystal molecule copper phthalocyanine-3,4',4'',4'''-tetrasulfonic acid tetrasodium salt (CuPcTs). Reprinted with permission [25]. Copyright 2015, American Chemical Society.

fiber-shaped supercapacitors with remarkable volumetric capacitance as high as 202 F cm^{-3} and extraordinary high-rate performance. Generally, electrochemical and electrical properties of self-crosslinked CPHs can be remarkably enhanced due to the absence of non-conductive frameworks and crosslinkers. However, a self-crosslinking strategy is not versatile for all CPs and usually accompanies with harsh treatment (such a supercritical CO_2 drying and condensed acid treatment), hindering it from wider application.

In addition with developing pure CPHs without adding crosslinkers, much efforts have been devoted to develop novel synthesis method towards 3D CPHs. For instance, Zhang and co-workers [52] proposed a PPy/PVA interpenetrating network through vapor-phase polymerization of pyrrole. An all-solid-state polymer supercapacitor (ASSPS) was then fabricated via sandwiching the PVA/ H_2SO_4 film between two pieces of the PPy/CPH film. The ASSPS is mechanically robust and flexible with a tensile strength of 20.83 MPa and a break elongation of 377% owing to the strong hydrogen bonding interactions among the layers and the high mechanical properties of the PPy/CPH. Besides, this device exhibits maximum volumetric specific capacitance of 13.06 F cm^{-3} and energy density of $1160.9 \text{ μWh cm}^{-3}$. In particular, Chu and his co-workers [53] built 3D interconnected PANI/phytic acid CPHs for high performance SSCs via electrochemical polymerization in the absence of chemical oxidative initiators. With 0.8 V potential (vs saturated

calomel electrode) applied on gold interdigital patterns, 3D CPHs consisting of interconnected nanoparticles can be sequentially constructed. Notably, since the polymerization is initiated by electrochemical potential, the utilization of chemical initiator can be effectively sidestepped. Due to the high conductivity (0.43 S cm^{-1} at room temperature) and improved interfaces between electronic transport phase and ionic transport phase, flexible solid-state micro-supercapacitors based on this hydrogel deliver high areal capacitance of 135.9 mF cm^{-2} and considerable energy density of 49.9 μWh cm^{-2} at 0.4 mW cm^{-2} . Table 1 summarizes recently reported CPHs for SSCs electrodes and their electrochemical performance.

2.1.2. 3D CPs/carbon composite for SSCs

As seen from the above discussion, 3D interconnected hydrogels based on CPs have been extensively explored for the fabrication of solid-state energy storage in supercapacitors. It can be clearly concluded that CPHs hold great promise for the fabrication of high performance flexible SSCs attributed to their considerable flexibility, interconnected 3D networks and high intrinsic pseudo-capacitance. Nevertheless, the conductivity of CPHs is relatively low (generally in the order of 10^{-2} to $10^{-1} \text{ S cm}^{-1}$). Besides, the doping and de-doping process of CPs usually leads to structure collapse of 3D networks of CPHs, which will deteriorate cycling stability of supercapacitors. In this

Table 1
Synthetic routes and performance of typical CPHs appeared in recent reports.

CPHs	Synthetic route	Conductivity (S cm ⁻¹)	Strength	Capacitance	Cycling stability (10000 cycles)	Energy density (Power density)	References
PANI/PVA/GA	In-situ polymerization	/	0.35 MPa at 300% tensile strain	488 mF cm ⁻² at 0.2 mA cm ⁻²	93% with 7000 cycles	42 μWh cm ⁻² (160 μW cm ⁻²)	[45]
PANI/ABA/PVA	Solution polymerization	0.1	5.3 MPa at 250% tensile strain	1350 F g ⁻¹ at 1 A g ⁻¹	~86% with 1000 cycles	13.6 Wh kg ⁻¹ (105 W kg ⁻¹)	[46]
PANI/AOAI	Solution polymerization	0.15	11 kPa with 112% elongation	919 F g ⁻¹ at 1 A g ⁻¹	90% with 1000 cycles	13.1 Wh kg ⁻¹ (89 W kg ⁻¹)	[47]
PANI/Phytic acid	Solution/biphasic polymerization	0.23	/	480 F g ⁻¹ at 0.2 A g ⁻¹	~83%	/	[27]
Ppy/Phytic acid	Liquid phase interfacial reaction	0.5	/	380 F g ⁻¹ at ~0.2 A g ⁻¹	~90% with 3000 cycles	/	[48]
PANI/ATMP	Solution polymerization	0.35	/	422 F g ⁻¹ at 0.2 A g ⁻¹	~93% with 2000 cycles	/	[44]
Ppy/CuFeTs	Solution polymerization	7.8	/	400 F g ⁻¹ at 0.2 A g ⁻¹	/	/	[25]
PEDOT:PSS/Fe ³⁺	Solution polymerization	0.05	0.176 MPa at 63.7% tensile strain	/	/	/	[49]
PANI	Self-crosslink strategy	/	6.0 kPa at 15% compressive strain	~750 F g ⁻¹ at 1 A g ⁻¹	/	/	[50]
PEDOT:PSS	Sulfuric acid treatment	8.8	280 MPa at 14.6% tensile strain (dehydrated fiber)	202 F cm ⁻³ at 0.54 A cm ⁻³	~100%	/	[51]
PANI/Phytic acid	Electrochemical polymerization	0.43	/	311 F g ⁻¹ at 1 A g ⁻¹	~76%	49.9 μWh cm ⁻² (400 μW cm ⁻²)	[53]
Ppy/PVA	Vapor-phase polymerization	/	20.83 MPa with 377% elongation	13.06 F cm ⁻³ at 5 mA cm ⁻³	86.3%	1160.9 μWh cm ⁻³ (4000 μW cm ⁻³)	[52]

context, it is of great necessity to improve the conductivity of CPs based materials serve as supercapacitor electrodes.

As a typical electrode material, carbonaceous materials with different state of aggregation including carbon nanotubes (CNTs), graphene, carbon film and hierarchical porous carbon (HPC) have been exploited in the fabrication of high performance supercapacitors attributed to high conductivity and unique porous structure. Since energy storage of carbonaceous materials mainly stems from EDLC mechanism, they deliver limited specific capacitance. In this regard, CPs could be rationally polymerized onto 3D carbonaceous frameworks thus better conductivity can be obtained. Besides, specific capacitance can be simultaneously enhanced compared with pristine carbonaceous materials due to the introduction of pseudo-capacitance.

2.1.2.1. SSCs based on 3D CNT/CP composites. Since the seminal work nearly three decades ago by Iijima [54], CNTs have become the focus of considerable research especially in the field of flexible electronics [55–57]. Generally, CNTs can afford limited capacitance when utilized as supercapacitor electrode materials attributed to low specific surface area. In this regard, CPs can be included into CNTs to enhance electrochemical capacitance by virtue of high intrinsic pseudocapacitance. Additionally, CNTs can naturally construct an interconnected 3D networks due to its high length-diameter ratio, thus it can be used as frameworks or polymerization templates for CPs.

To date, many different strategies have been developed for the preparation of high performance 3D flexible CNTs/CP networks. Among various CPs, polyaniline is the most popular one for inclusion of CNTs attributed to its variable oxidation state, low cost and easy synthesis. Fan et al. [58] developed a facile method for the preparation of a 3D hierarchical nanocomposite of vertical PANI nanorods aligned on the surface of functional multiwall carbon nanotubes (FMWNTs) by in situ polymerization of PANI on the surface of FMWNTs (as shown in Fig. 4). It is demonstrated that a uniform PANI shell can be easily formed on the surface of FMWNTs while in situ synthesis of PANI on the non-functionalized MWNTs leads to the formation of a mixture of mostly PANI nanofibers. Morphology characterization of PANI/FMWNTs composites with different reaction time indicates a ‘seed growth’ mechanism. Initial polymerization of aniline ions tends to form seeds on the surface of FMWNTs. Then, PANI grows along the seeds and vertically aligned PANI nanorods on the FMWNTs sidewall are produced. Consequently, this 3D PANI/FMWNTs composites exhibit a high specific capacitance of 568 F g⁻¹ at the current density of 10 A g⁻¹, which is larger than that of pure FMWNTs. Similarly, Cai and co-workers [59] successfully incorporated PANI with aligned CNTs, which delivers large capacitance of 274 F g⁻¹ and can be further applied in the fabrication of fiber-shaped microsupercapacitors.

Since the vast majority of flexible solid-state supercapacitors share a laminated structure in which solid-state electrolyte is sandwiched between two electrode films, it is of great necessity to assemble electrode into flexible freestanding films. In this context, CTNs can be incorporated with CPs for the fabrication of freestanding films. Meng et al. [60] reported a novel method to prepare paper-like CNT/PANI composites by using CNT network as the template. Compared with the conventional brittle CNT/PANI composites, these paper-like composites were much thin and flexible (Fig. 5a). As a result, this composite paper exhibits a high conductivity (150 S cm⁻¹) and large specific capacitance of 424 F g⁻¹. This work opened up an avenue for the design and fabrication of paper-like films consisting of CNT and CPs. Similarly, Zhang and co-workers [61] prepared multi-walled carbon nanotube (MWCNT)/PANI composite films through in situ electrochemical polymerization of aniline solution containing different MWCNT contents. The resultant film also exhibits large specific capacitance, better power characteristic, and good cyclic stability, which can be further utilized for SSCs.

In addition, with CNTs, other carbonaceous tubular materials featuring large length-diameter ratio such as carbon nanofiber, graphite

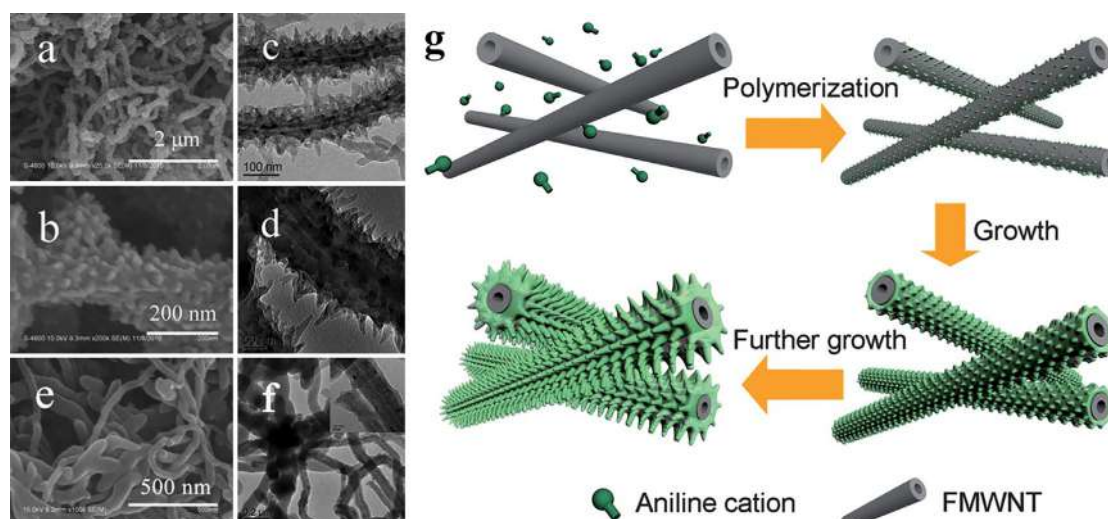


Fig. 4. (a, b) SEM and (c, d) TEM images of 3D PANI-FMWNTs nanocomposites. (e) SEM and (f) TEM images of PANI-MWNTs nanocomposites. (g) Schematic illustration of the formation of PANI-FMWNTs nanocomposite with vertical PANI nanorods on FMWNTs. Reprinted with permission [58]. Copyright 2012, Springer.

nanofibers and hierarchical carbon tubular nanostructures (*hCTNs*) have also been used as polymerization template for CPs. Typically, He et al. synthesized long, ordered and needle-like PANI nanowires onto graphitized electrospun carbon fibers (GECFs) to prepare PANI/GECF composite cloths as electrode material for supercapacitors (shown in Fig. 5b). These flexible PANI/GECF composite cloths with 3D hierarchical micro/nano-architecture can be directly made into electrodes without any conductive additives and binders, which displayed a high specific capacitance of 976.5 F g^{-1} at the current density of 0.4 A g^{-1} . In particular, Yan and co-workers [62] homogeneously deposited PANI nanoparticles onto the surface of electrospun carbon nanofiber (CNF) serve as substrate via simple rapid-mixture polymerization. The resultant CNF/PANI paper delivered high specific capacitance of 638 F

g^{-1} , which is a potential low-cost candidate for use as flexible SSCs. Intriguingly, Zhang et al. [63] proposed a novel 3D carbonaceous structure called *hCTNs*, which is derived from one-step conversion of greenhouse gas CO_2 . This tubular structure possesses blood vessel like hierarchical structure, which facilitate electrolyte penetration and electron transfer. Chu et al. [26] then in situ polymerized PANI nanoparticles onto the surface of this tubular structure, 3D hierarchical *hCNTs*/PANI composites thus comes into formation. Notably, these *hCNTs*/PANI composites can be easily synthesized onto stainless steel springs to prepare a highly stretchable electrode (Fig. 5c). This work may give inspiration for the design and fabrication of novel stretchable devices.

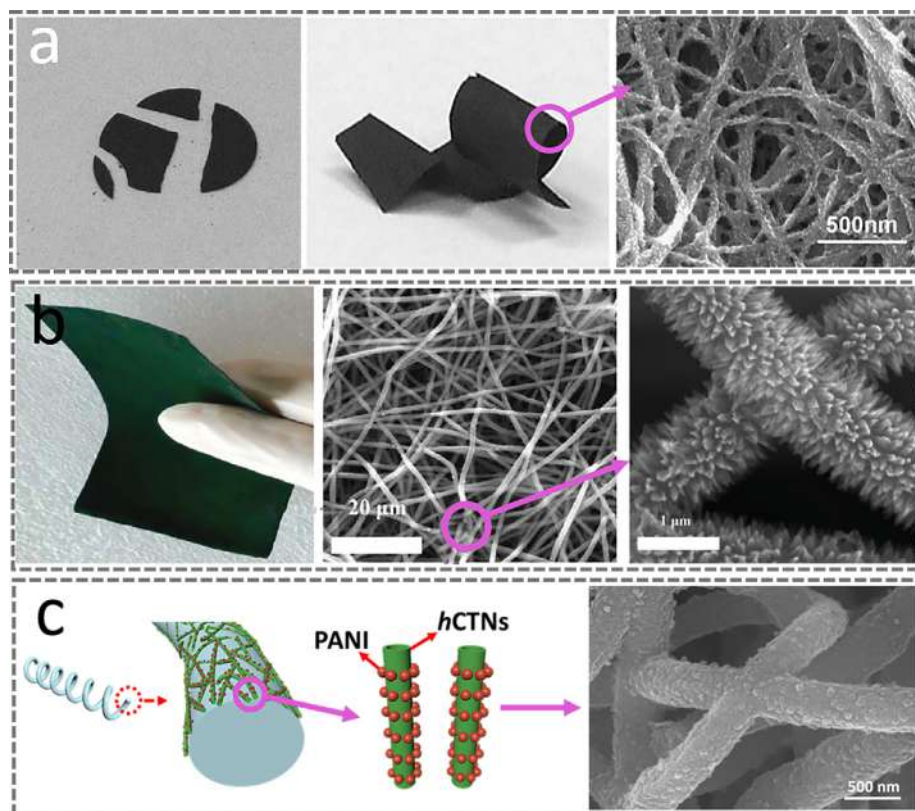


Fig. 5. (a) Brittle CNT paper/PANI tablet and flexible buckypaper/PANI composite. Reprinted with permission [60]. Copyright 2009, Elsevier Science Inc. (b) PANI/GECF (graphitized electrospun carbon fibers) cloth with PANI nanowires uniformly wrapped carbon fibers. Reprinted with permission [64]. Copyright 2012, the Royal Society of Chemistry. (c) In situ synthesized 3D hierarchical PANI/*hCTNs* structure for a highly stretchable supercapacitor electrode. Reprinted with permission [26]. Copyright 2019, Elsevier Science Inc.

2.1.2.2. SSCs based on 3D Graphene/CP composites. Graphene, a 2D monolayer of sp²-bonded carbon atoms, has attracted increasing attention in electrochemical energy storage attributed to high electrical conductivity, mechanical flexibility as well as excellent chemical stability. However, it is still baffling for researchers to achieve the high theoretical specific capacitance of graphene (~550 F g⁻¹) due to the restacking of individual graphene sheet. To address this problem, ultrasonic assisted method or various spacers (e. g. CNTs, carbon nanoparticles, metal ions, and polymers). Inclusion of CPs with graphene affords a smart maneuver since this method can hinder restacking of graphene while increase specific capacitance synchronously. Therefore, Wu et al. [65] reported a composite film of chemically converted graphene (CCG) and polyaniline nanofibers (PANI-NFs) can be prepared by vacuum filtration the mixed dispersions of both components. Morphology characterization reveals the composite film has a 3D layered structure, in which PANI-NFs are sandwiched between CCG layers. Due to the introduction of graphene layers, electrical conductivity of PANI-NFs can be remarkably enhanced to a high level of $5.5 \times 10^2 \text{ S cm}^{-1}$. The composite film also exhibits large electrochemical capacitance of 210 F g⁻¹ along with improved electrochemical stability and rate performance. Similarly, Xu and co-workers [66] in-situ synthesized PANI nanowires aligned vertically on the surface of graphene oxide (GO), thus 3D hierarchical composite comes into formation. Amazingly, the hierarchical nanocomposite possessed higher electrochemical capacitance and better stability than each individual component as supercapacitor electrode materials, showing a synergistic effect of PANI and GO. Recently, Zou et al. [67] demonstrated a mechanically robust double-crosslinked network consisting of functionalized graphene and PANI by polymerization of aniline in a confined functionalized graphene (PGH) hydrogel framework. As a result, symmetric supercapacitor based on this stiff hydrogel achieve a superior areal specific capacitance of 3488.3 mF cm⁻² and a volumetric specific capacitance of 872 F cm⁻³, remarkable rate capability, and excellent cycling stability. In addition to PANI, other CPs such as PPy and PEDOT have also been coupled with graphene in order to obtain 3D networks. For instance, Oliveira et al. [68] reported high-quality composites for supercapacitors through interfacial/in situ oxidative polymerization of polypyrrole in the presence of functionalized graphene sheets, which delivers higher storage capacity (277.8 F g⁻¹) than each individual film due to the synergistic effect of PPy and graphene.

2.1.2.3. SSCs based on 3D CNT/Graphene/CP composites. Inclusion of CPs with CNT/graphene composites is also demonstrated to be a promising method to enhance electrochemical performance. CNTs with large length-diameter ratio serve as both spacers hindering restacking of graphene layers and connectors bridging two separated graphene layers to construct interconnected electron transfer paths. Additionally, in situ polymerized CPs can be doped by carboxylated CNTs during polymerization process. Therefore, many research groups have investigated CNT/graphene/polyaniline ternary composites.

Fan et al. [69] recently reported 3D conductive PANI/rGO/MWNTs network for high performance SSCs. This 3D network is fabricated through a typical rapid-mixture polymerization of aniline in the presence of MWNTs/GO hybrid film obtained by vacuum filtration, followed by reduction using 55% hydroiodic acid. In this hybrid system, MWNTs on the one hand inhibit the aggregation of 2D GO, on the other hand bridge the gaps between reduced GO to form a three-dimensional conductive network, thus efficient conductive pathways can be constructed within this 3D networks. Consequently, the PANI/rGO/MWNTs film exhibits high specific capacitance of 498 F g⁻¹ at 0.5 A g⁻¹ as well as excellent long cycle life of 95.8% capacitance retention over 3000 cycles. Similarly, Faraji and co-workers developed PANI/graphene/MWCNTs plastic films employing polyphenylene sulfide (PPS) polymer matrix [70]. The resultant freestanding film shows comprehensively excellent mechanical and electrochemical properties

for the fabrication of flexible SSCs. In addition with PANI, other conducting polymers such as polypyrrole [71], poly(3,4-ethylenedioxythiophene) [72] have also been applied to build ternary 3D CP/CNT/graphene networks, which exhibit promising electrochemical performance.

2.1.2.4. SSCs based on other 3D carbon/CP composites. Graphene and CNTs are surely two starring materials in the big family of carbon materials. However, there are yet still numerous other members existed in this big family such as active carbon [73], onion like carbon [74], hierarchical porous carbon (HPC) [75], biomass derived carbon [76,77] and carbide derived carbon (CDC) [78], which could possibly construct 3D conductive scaffolds for CPs and consequently enhance electrochemical performance of CPs. In this context, Miao and his co-workers developed a freestanding 3D HPC materials with high specific surface area of 320 m²/g through a facile phase separation method [79]. PANI was then in situ chemical polymerized onto HPC frameworks to decorate the 3D HPC. As a result, the HPC/PANI composites exhibit much higher specific capacitance up to 290 F g⁻¹ at 0.5 A g⁻¹ than that of HPC (198 F g⁻¹). The resultant supercapacitor delivers high energy density of 9.6 Wh kg⁻¹ at 223 W kg⁻¹ along with good cycling stability. Liu et al. reported a convenient and inexpensive "skeleton/skin" strategy to prepare carbon aerogel-polyaniline (CA-PANI) hybrid materials with vertically aligned pores [80]. This hybrid composites exhibits an extraordinary rate capability with a high capacity retention (95%) when the current density is increased from 1 to 100 A g⁻¹. Similarly, He et al. fabricated a 3D ordered honeycomb-like nitrogen-doped carbon (HNC) via the sacrificial template method [81]. This 3D carbon skeleton exhibits high specific surface area of 1056 m² g⁻¹ as well as ordered structure. The HNC/PANI shows excellent performance as high as 686 F g⁻¹ at 1 A g⁻¹ along with the good rate performance and superior cyclic stability, which could be potentially used in SSCs.

2.2. 3D polymer electrolytes for SSCs

Solid-state electrolyte is another crucial component of SSCs, which plays an unambiguously important role in determining electrochemical performance of SSCs. Compared with liquid electrolytes, solid-state electrolytes have higher reliability and wider operation temperature. Importantly, usage of separator and electrolyte leakage problem can be effectively avoided when solid-state electrolytes are employed. In 3D polymer electrolytes, the ions migration mechanism below or at room temperature can be ascribed to the direct transport via polymer chain segmental motions. For example, in the proton conducting 3D polymer electrolyte, the proton transportation is restricted to the amorphous phase of solvating polymers, where the polymer molecules are free to move. Therefore, proton conduction by segmental motion is only possible above the glass transition temperature (*T_g*) of the polymer. In the amorphous phase, the polymer side chains can vibrate to a certain extent, thus reducing or eliminating the distance for proton conduction [82]. The most widely used solid-state electrolytes in SSCs are gel electrolytes, which consists of 3D polymer framework as the host of solvated ions, an organic/aqueous solvent serve as plasticizer and a typical supporting electrolytic salt. 3D polymeric electrolytes of SSCs must exhibit the following properties: (i) high ionic conductivity at room temperature; (ii) low electronic conductivity; (iii) good mechanical properties or dimensional stability; (iv) high chemical, electrochemical, and environmental stability; and (v) sufficient thin-film processability. As shown in Fig. 6, various polymers with soft and flexible molecular chains such as poly (vinyl alcohol) (PVA) [53,83], poly (ethylene oxide) (PEO) [84], polyarylate (PAA), polyacrylonitrile (PAN), polyacrylamide (PAM), poly(methyl methacrylate) (PMMA) [85] and their derivatives are the most commonly used polymer for the preparation of gel electrolytes. Additionally, naturally occurring polymeric materials such as cellulose [22,86], chitin and chitosan [87]

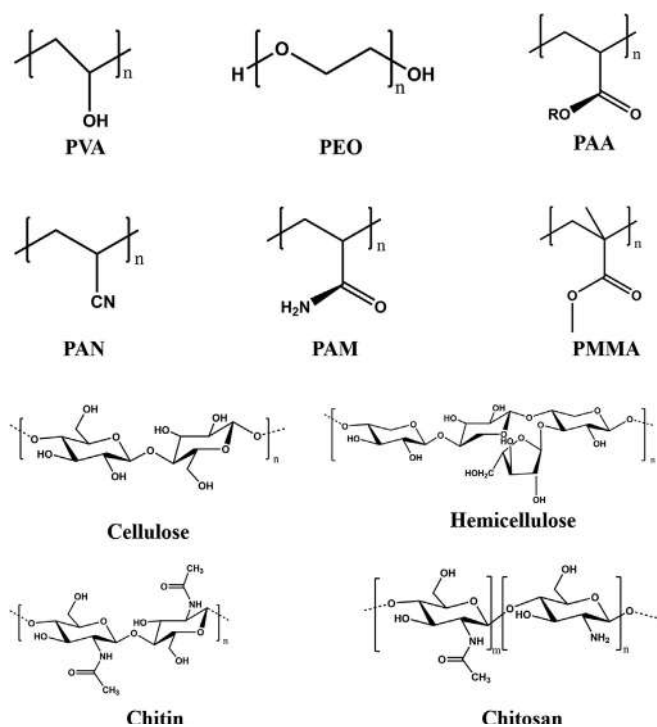


Fig. 6. Molecular structures of various polymer matrix used in the preparation of gel polymer electrolytes for SSCs.

emerged as a starring maneuver for gel electrolytes attributed their low cost and easy accessibility. Inorganic solid-state electrolyte such as $\text{Li}_{2.94}\text{PO}_{2.37}\text{N}_{0.75}$ electrolyte film [88], phosphotungstic acid/ $\text{Al}_2(\text{SO}_4)_3 \cdot 18\text{H}_2\text{O}$ [89], and $\text{Li}_2\text{S-P}_2\text{S}_5$ [90] have also been reported for the fabrication of thin film SSCs, which will not be discussed in detail in this review because herein we mainly focus on 3D polymer based electrolytes. Generally, 3D polymer gel electrolyte can be divided into four categories according to the properties of electrolytic salt: (i) proton conducting polymer gel electrolytes; (ii) alkaline gel polymer gel electrolytes; (iii) lithium ion polymer gel electrolytes; (iv) other polymer gel electrolytes.

2.2.1. Proton conducting gel polymer electrolytes

Proton conducting polymer gel electrolytes have been widely employed for the fabrication of SSCs because protons have high mobility and therefore facilitate ultrafast charging-discharging process. PVA/ H_3PO_4 proton conducting polymer blend was fabricated as a pioneer with an ionic conductivity of $2.2 \times 10^{-5} \text{ S cm}^{-1}$ [91]. Since then various types of proton conducting polymer gel electrolytes have been explored to satisfy specific condition. Notably, conducting polymers can be easily doped by proton acids, therefore proton conducting polymer gel electrolyte are often utilized when conducting polymer electrode is employed [45,52,53,92]. For a typical fabrication of proton conducting polymer gel electrolytes, polymer matrix and proton donor source are often blended in a polar solvent with elevated temperature and a uniform gel electrolyte can thus come into formation. H_2SO_4 , H_3PO_4 and heteropolyacids are commonly used as proton donors for the fabrication of proton conducting polymer gel electrolytes. Currently, a series of proton conducting polymer gel electrolytes including PVA/ H_2SO_4 , PVA/ H_3PO_4 [93], PVA/ H_3PO_4 /silicotungstic acid [94,95], PVA/ H_3PO_4 / H_3BO_3 [96], Methylcellulose/PVA/ NH_4NO_3 [97], and starch-chitosan/ NH_4Cl [98] have been successfully demonstrated for SSCs. Recently, Naik et al. [99] reported an ease and novel method to synthesize CeO_2 nanoparticles in PVA polymer matrix, which shows proton conductivity of the order of $10^{-3} \text{ S cm}^{-1}$. This ceria filled PVA proton conducting polymer electrolyte can be further utilized in portable and

flexible energy storage devices. Vijayakumar and co-workers [100] developed a new conceptual water-in-acid gel polymer electrolyte towards SSCs. For a typical fabrication of polyelectrolyte gel polymer electrolyte (PGPE), [2-(acryloyloxy) ethyl] trimethylammonium chloride (AOETMA) and 2-Hydroxyethyl methacrylate (HEMA) were copolymerized through UV-light-assisted synthesis. Consequently, the copolymer film was immersed in concentrated H_3PO_4 until equilibrium swelling. The resultant PGPE exhibits high proton conductivity of $9.8 \times 10^{-2} \text{ S cm}^{-1}$ at ambient temperature. The PGPE based solid-state PANI supercapacitors deliver high specific capacitance of 385 F g^{-1} along with good cyclic stability. To improve specific capacitance of SSCs, pseudocapacitance can be introduced through adding some typical redox-active additives into gel polymer electrolytes. As an example, Pan et al. [24] prepared an effective redox-active gel electrolyte by adding 2-mercaptopyridine (PySH), an electrochemical active compound, to the PVA/ H_3PO_4 electrolyte for the fabrication of fiber-shaped SSCs (shown in Fig. 7a). As a result, fiber-shaped SSCs based on this PVA- H_2SO_4 -PySH demonstrate distinct redox characteristics and longer discharge time compared with pure PVA- H_2SO_4 . Similarly, redox-active p-benzenediol [23] and methylene blue [101] can be added into proton conducting gel polymer electrolyte to enhance capacitance (shown in Fig. 7b and c).

2.2.2. Alkaline gel polymer electrolytes

Alkaline gel polymer electrolytes have attracted increasing attention due to their potential application in solid-state alkaline rechargeable batteries and SCs. Currently, numerous alkaline gel polymer electrolytes have been developed for high performance SSCs, including PEO/ $\text{KOH}/\text{H}_2\text{O}$ [102], PVA/ $\text{KOH}/\text{H}_2\text{O}$ [103,104], PVA/PAA/ KOH [105], PAAK/ $\text{KOH}/\text{H}_2\text{O}$, poly(epichlorohydrin-co-ethyleneoxide) P(ECH-co-EO)/ $\text{KOH}/\text{H}_2\text{O}$ [106], and PVA/sodium polyacrylate (PAAS)/ $\text{KOH}/\text{H}_2\text{O}$ [107]. Recently, Hu et al. [108] reported a flexible and low temperature resistant double network alkaline gel polymer electrolyte, in which KOH is served as both ionic donor and cross-linking agent. This double-network physical cross-linked hydrogel consisting of PVA/ κ -carrageenan is synthesized through a green physical route. Intriguingly, the resultant GPE exhibits excellent tensile stress (2.22 MPa) along with extraordinary ionic conductivity (0.21 S cm^{-1}). Activated carbon based on this GPE also delivers high specific capacitance (470 F g^{-1} at 0.5 A g^{-1}) and good cycling life (95% capacitance retention over 2000 charge/discharge cycles). Ma et al. [109] prepared a PVA/ $\text{KOH}/\text{K}_3[\text{Fe}(\text{CN})_6]$ gel electrolyte for SSCs with activated carbon used as electrodes. It is found that the highest conductivity of 45.56 mS cm^{-1} can be reached with $\text{K}_3[\text{Fe}(\text{CN})_6]$ content of 0.04 g. Due to the existence of $[\text{Fe}(\text{CN})_6]^{3-}$ and $[\text{Fe}(\text{CN})_6]^{4-}$ ion pair, reversible redox reaction can be effectively introduced and specific capacitance of SSCs can be thus enhanced. Similarly, p-phenylenediamine [110] and KI [111,112] can also be added into PVA/ KOH systems for the same purpose.

2.2.3. Lithium ion gel polymer electrolytes

Lithium ion electrolyte are commonly utilized in Li ion batteries as well as SCs. Additionally, recent proliferation of Li ion capacitors also boosts lithium ion electrolyte. Up to now, multifarious Li ion gel polymer electrolyte such as PVA/ LiCl [113], PVA/ LiClO_4 [114], cellulose/PVA/ Li_2SO_4 [22], poly(ether ether ketone) PEEK/PVA/ LiClO_4 [115], lithium bis(trifluoromethanesulfonyl)imide LiTFSI/PMMA [116], LiPAA/PAM [117], and poly(glycidyl methacrylate)/ LiClO_4 [118] have been developed to satisfy specific conditions. Virya et al. [117] recently reported lithium ion gel polymer electrolyte consisting of lithium polyacrylate (LiPAA) and polyacrylamide (PAM). The LiPAA was prepared through ion exchange method by adding stoichiometric amount of LiOH powder into 5 wt% poly(acrylic acid) solution for neutralization. Sequentially, LiPAA-PAM electrolyte precursor solutions were prepared by mixing 5.5 wt% LiPAA solution and 3 wt% PAM solution to form an electrolyte film with fixed weight ratio. Consequently, the LiPAA-PAM electrolyte achieved an ionic conductivity of

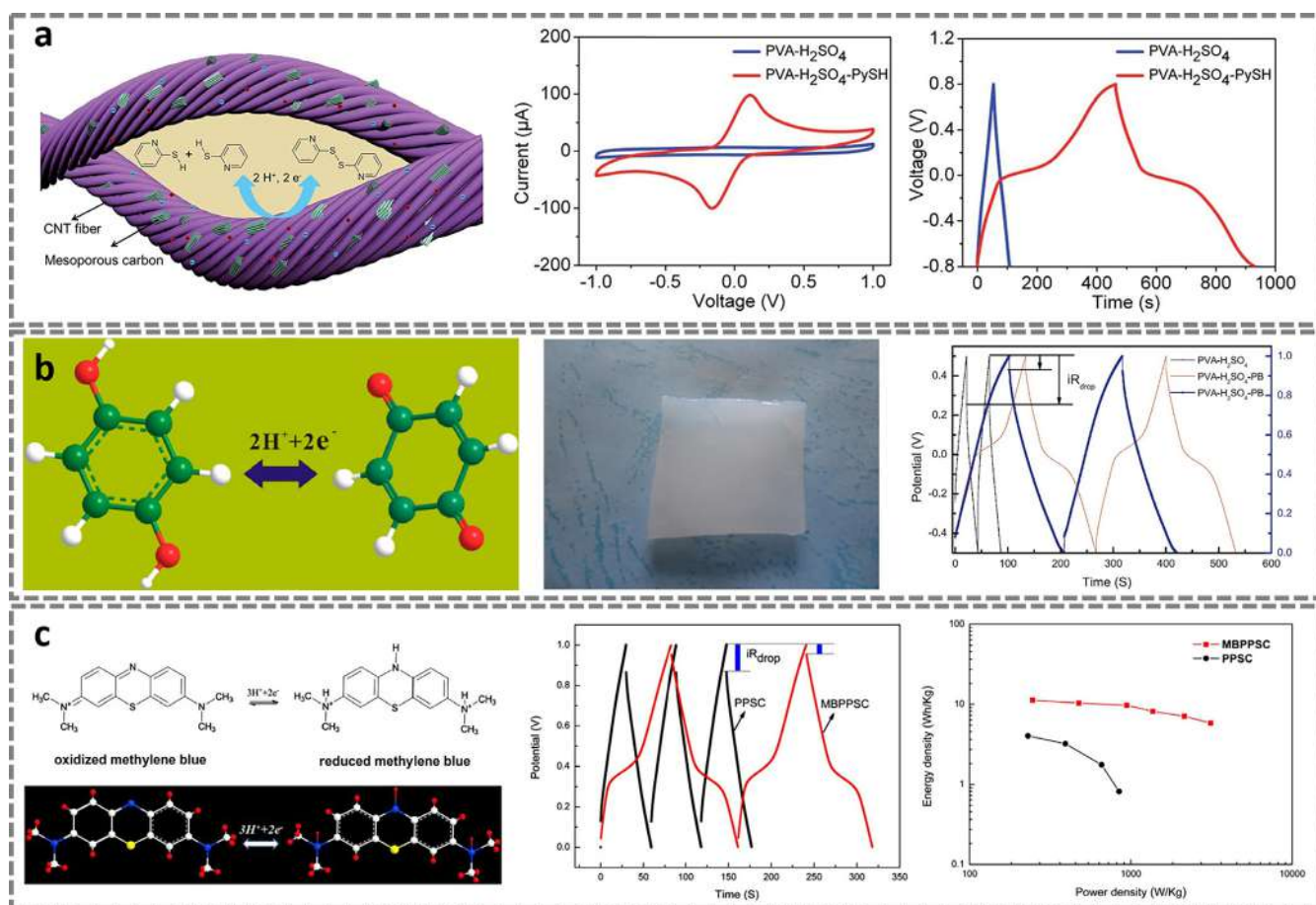


Fig. 7. (a) Schematic illustration of fiber-shaped supercapacitors with 2-mercaptopyridine/PVA/H₂SO₄ gel electrolyte. Reprinted with permission [24]. Copyright 2015, the Royal Society of Chemistry. (b) A novel redox-mediated gel polymer PVA/H₂SO₄/P-benzenediol electrolyte for high performance supercapacitor. Reprinted with permission [23]. Copyright 2012, Elsevier Science Inc. (c) PVA-PVP-H₂SO₄-MB (methylene blue) gel polymer electrolyte for quasi-solid-state supercapacitor. Reprinted with permission [101]. Copyright 2013, Wiley-VCH. (For interpretation of the references to colour in this figure legend, the reader is referred to the web version of this article.)

$13.8 \pm 2.4 \text{ mS cm}^{-1}$, which is even higher than many aqueous-based neutral pH polymer electrolytes. To demonstrate application potential of LiPAA-PAM electrolyte, the flexible electrolyte film was assembled into solid-state supercapacitor cells. These solid-state cells demonstrated wide voltage window (1.5 V), good cycle life ($> 10,000$ cycles), and excellent rate capability (up to 500 mV s^{-1} in cyclic voltammetry). Tang et al. [118] developed a hierarchical porous carbon (HPC) doped gel polymer electrolyte for asymmetric SSCs. This gel polymer electrolyte was obtained through adding DMF-LiClO₄, HPC in glycidyl methacrylate (GMA), followed by photopolymerization of GMA. Intriguingly, the interconnected microtunnels in HPC microspheres could shorten the pathway for ions transfer and then improve the conductivity. The resultant SSCs could therefore exhibit remarkable electrochemical performance.

2.2.4. Other ion gel polymer electrolytes

In addition to the abovementioned gel polymer electrolytes, numerous other types of polymer electrolytes have also been exploited for the design and fabrication of SSCs. For instance, Yang and co-workers [119] developed a new type of gel polymer electrolyte, in which poly(vinylidene fluoride-hexafluoro propylene) P(VDF-HFP) serves as polymer matrix, ionic liquid (1-ethyl-3-methylimidazolium tetrafluoroborate, EMIMBF₄) serves as the supporting electrolyte. Besides, 1 wt% amount of GO was homogeneously incorporated with this ion gel acting like an ion 'highway' to facilitate the ion transport. As a result, a dramatic improvement in ionic conductivity of about 260% can be

clearly observed compared with that of pure ion gel. Tu et al. [120] recently reported a PVA/Li₂SO₄/1-butyl-3-methylimidazolium iodide (BMIMI) composite electrolyte for activated carbon-based flexible supercapacitor. In this hybrid system, BMIMI acts as both plasticizer and pseudocapacitance donor. Due to the high ionic conductivity (46.0 mS cm^{-1}) and Faradic reactions of I-based gel electrolyte, electrode-specific capacitance (active carbon electrode) of SCs with PVA-Li₂SO₄-BMIMI electrolyte is calculated to be higher (384.1 F g^{-1}) than that of SCs with PVA-Li₂SO₄-BMIMCl (1-butyl-3-methylimidazolium chloride) electrolyte (139.1 F g^{-1}).

3. 3D polymers for solid-state lithium-ion batteries

3.1. 3D polymer composite electrodes for ASSLIBs

Compared to the traditional 2D electrodes like copper foil or aluminum foil current collectors, 3D structured electrodes offer highly efficient charge delivery, even in thick electrodes with practical levels of mass loading. In principle, polymers are already studied heavily for the ASSLIBs electrolyte phase to produce all-solid systems, so it is necessary for polymer-based 3D electrodes to form favorable interface with solid-state electrolyte or active material for fast ion transport. Additionally, other desirable features of polymers such as flexibility may take consideration for the ability to adapt many modules and configuration (e.g., wearables and unique folding for improved packing efficiency). Moreover, the improved transport may demand thicker

Table 2
Summary of characteristic and performance metrics of representative 3D composite electrodes.

3D electrodes	Active material (%)	Fabrication method	Gravimetric performance (mAh g ⁻¹)	Rate performance (mAh g ⁻¹)	Capacity retention	Refs.
Polyaniline/Si	75	In situ polymerization	550	1000 at 8.3 A g ⁻¹	86% 1000 cycles*	[123]
Polypyrrole/Fe ₃ O ₄	85	Co-precipitation	1100	700 at 2 C	79% 50 cycles*	[124]
Polypyrrole/LFP	86	In situ polymerization	133	60 at 30 C	75% 500 cycles*	[125]
PEO/PEDOT	64	Solution self-assembly	25	—	—	[126]
GF/PI	65	One-step self-assembly	240	120 at 1 A g ⁻¹	80.4% 1000 cycles*	[16]
LTO/GF//LFP/GF	88	CVD, hydrothermal	117	135 at 200 C	90% 500 cycles*	[127]
N-doped GF	80	Freeze-drying, CVD	1057	150 at 10 C	69.7% 150 cycles*	[128]
PAQS/graphene	80	Freeze-drying	156	80 at 30 C	72% 1000 cycles*	[129]
TBA-TEVS/Si	74	Radical polymerization	2991.9	1750 at 10 C	81% 100 cycles*	[130]
Li/PI/ZnO	85	Electrospinning, ALD	2070	—	86% 100 cycles*	[17]
Li/PMF	—	Molten self-assembly	—	76 at 4 C	85% 1000 cycles*	[131]
Li/PMMA	—	In-situ deposition	—	80 at 4 C	75% 200 cycles*	[132]
SAPs/NiO/Ni	80	Freeze-drying, self-assembly	1152	440 at 4 C	93% 200 cycles*	[133]
Poly[Ni(CH ₂ -salen)]/LFP	93	Solution self-assembly	153	50 at 10 C	96% 150 cycles*	[134]
PTAm/SWNT	95	Solution self-assembly	—	135 at 20 C	67% 1000 cycles*	[135]
PFA/PVA/Si	95	In-situ polymerization	2916.5	1750 at 0.8 A g ⁻¹	73.6% 300 cycles*	[136]
PVDF-HFP/Cu	80	Solution self-assembly	153	—	99% 300 cycles*	[137]

* LFP, LiFePO₄; CVD, chemical vapor deposition; ALD, atomic layer deposition; PMF, poly-melamine-formaldehyde; PAB, poly(1,3-diethylbenzene); PTAm, poly(2,2,6,6-tetramethylpiperidinyloxy-4-yl acrylamide); SWNT, single-walled carbon nanotube; PFA, poly(furfuryl alcohol); PVA, polyvinyl alcohol; * Present these properties tested in liquid electrolyte.

architecture, which would further increase energy density without loss to power density. However, it is difficult for a single polymer material to directly applied as an electrode. Thus, the 3D structure in the electrode material is mainly composed of the polymer/carbon composite or novel organic electrode with conductive polymer. In this part, we will systematically review the 3D polymer composite electrode for ASSLIBs, including the polymer materials selection, 3D composite structure processing design and correlation enhancement mechanism. Table 2 summarizes characteristic and performance metrics of representative 3D composite electrodes for ASSLIBs.

3.1.1. Cathode

In the conventional battery cathodes, active particles such as lithium iron phosphate (LFP) are connected by the binder system that consists of conductive carbon (CC) additives and nonconductive binder polymer to realize the construction of percolative pathways. This binder system often becomes the bottleneck for development of higher-performance lithium ion batteries mainly due to two important issues. One is the difficulty to achieve both high electronic and ionic conductivity and the other is the poor dispersion of electrode component, especially when nano/micro-sized materials are involved. Moreover, the insulative polymer binders could not only decrease the energy density, but also blocks the electron transport pathways. For the maximization of the energy density, pathways within the electrode for both electrons and ions must be low-resistance and continuous, reaching the entire volume of the battery. While in conventional electrodes, conductive additive carbon particles are randomly distributed and tend to aggregate during electrochemical reactions, thus poor contacts of electronic connections may occur. In Liquid-LIBs, ionic conductivity is increase by the wetting of porous regions of the electrode with the liquid electrolyte and is often limited by the electrode morphology. While for ASSLIBs, these pathways are limited by length, poor solid-solid interface between electrode and electrolyte.

To enhance the electrochemical performance of the ASSLIBs, the Li⁺ conductivity of the cathode should be paid attention. Due to the Li⁺ transportation in ASSLIBs is obviously different from that of commercial Liquid-LIBs, in which the Li⁺ transfers through liquid electrolyte between electrodes. In the ASSLIBs, the Li⁺ transportation among cathode active materials greatly restricted because these active materials particles in the cathodes phase generally do not directly contact with each other but are commonly bonded tightly by the binder such as polyvinylidene fluoride (PVDF). Only those active materials locate in

the interface between cathode and solid electrolyte can insert/extract Li⁺, resulting in relatively low specific capacity and high interface resistance during the electrochemical reaction process. In previous works, the solid electrolyte often mixed with the cathode materials to act as a Li⁺ ionic conductor during preparation, but only to form a discontinuous Li⁺ conductive network [121,122]. The construction of Li⁺ conductive network with 3D structures in the cathode is expected to be a powerful alternative to achieve high active material utilization rate. For a practical cathode in LIBs, several methods for constructing 3D conductive network architectures are recently proposed. Through these different elegant strategies, cathodes with high electronic and ionic conductivity which could facilitate the electron and Li⁺ transportation during cycling can be acquired.

One strategy that have been extensively investigated for 3D polymer composite electrodes is electronically conducting polymers, such as Polythiophene, Polypyrrole, Polyaniline and so on [42,138–141]. Of these, poly(3,4-ethylenedioxythiophene) (PEDOT) is the most promising candidates because of its excellent conductivity, chemical stability and processability. PEDOT is commercially available in an aqueous dispersion with poly(4-styrenesulfonic acid) (PSS), which helps solubilize PEDOT and compensated its charged backbone [142]. Unlike the CC particles, that are incorporated based on percolation thresholds, conductive polymers like PEDOT: PSS make up of most of the bulk conductive materials, leading to continuous electron transport pathways throughout the whole cathode. Another typically ignored problems is the specifically effective Li⁺ delivery in ASSLIBs cathodes. This can also be particularly addressed via the combination of a functional ionic conductive polymer like Polyethylene (PEO), Polyvinylidene Fluoride (PVDF) and Polyacrylonitrile (PAN) [143–146]. PEO is the most widely studied lithium ion-conductive polymer for lithium ion battery solid electrolytes. Its conductivity in the amorphous state arises from ion-dipole interactions between Li⁺ and lone pair electrons on PEO oxygen, along with its flexible chains that allow ion mobility.

As a representative example, Michael et al. [126] combined the electrically conductive PEDOT:PSS and lithium-conducting polymer PEO to form a dual conductor for 3D electrodes, which exhibited both high ionic (~10⁻⁴ S cm⁻¹) and electronic conductivity (~45 S cm⁻¹). In this 3D cathode, the PSS interacts favorably with PEO, destabilizing PEDOT to associate into highly branched, interconnected networks that allow for more efficient electronic transport despite relatively low concentrations. PEO could also be combined previously with another conducting polymer, poly(pyrrole), as a coating for ASSLIBs cathode

storage materials to successfully access greater capacity. Thus, Renáta Oriňáková et al. [147] adapted the PPy/PEG co-polymer to establish a more stable polymeric 3D structure, ultimately facilitate the solubility and insertion/extraction of the Li^+ ion in the matrix.

In principle, the cathodes in commercial LIBs are based on the inorganic active materials like graphite-based porous carbon materials, which have been widely adopted but still criticized in slow Li^+ migration, low theoretical capacities, structural instability, as well as large energy consumption for production. The advanced organic cathodes, especially conjugated carbonyl compounds, have been regarded as another novel strategy to replace traditional inorganic cathodes due to their high theoretical capacities, fast reaction kinetics, environmental sustainability, and structural diversity as well as insensitivity to the ion radius [148–150]. Generally, the organic electrode can be divided into three types (n-types; p-types and bipolar types). For n-types organics, the reaction is between the neutral state (N) and the negatively charged state (N^-), while for p-type is the neutral state (P) and positively charged state (P^+). The bipolar types can be either reduced to negatively state (B^-) or oxidized to positively state (B^+). In the electrochemical reaction process of organic electrodes, cation (Li^+) or anion (A^-) are necessary to neutralize the negative charge of N^- or the positive charge of P^+ , respectively. And then, Li^+ or A^- will migrate back from the electrode to the electrolyte. For many n-type organics, Li^+ can be substituted by other alkali metals (like Na^+ and K^+), which will not significantly affect the ion storage behavior of the material. This is greatly different from inorganic intercalation compounds, which are very sensitive to the radius of the cation [150]. In particular, conjugated carbonyl polymers with a stable skeleton and highly electroactive carbonyl groups, such as polyimide (PI), have received intense attention because of their significantly improved cycle life compared to small conjugated carbonyl molecules. However, the intrinsic electronic insulation of conjugated carbonyl polymer makes it very difficult to achieve high utilization efficiency in the common electrodes fabricated through the traditional physical mixing method despite a large amount of CC (> 30–60 wt%) used. Moreover, the inclusion of such large portions of electrochemically inert additives not only greatly compromises the electrochemical performance of the entire electrode but also makes the electrode unsuitable for the application in flexible energy storage devices. Therefore, it is critical to create a single binder-free and flexible polymer cathode simultaneously with high capacity, high rate capability, and long cycle life for ASSLIBs, which are essential for practical applications.

In this circumstance, Huang and his coworkers [16] firstly reported a 3D reduced graphene oxide/PI composites (GF-PI) through a one-step solvothermal strategy with simultaneous in situ polymerization of PI on the graphene surface, and the reduction of GO could be self-assembled into satisfactory 3D network structure (Fig. 8). This unique structure of the PI polymer throughout the graphene framework was mainly attributed to the π - π interaction between graphene and backbones of PI containing conjugated aromatic rings, which could facilitate fast ion diffusion and rapid electron transfer between graphene substrate and PI for the fast-redox reaction [151,152].

The application of 3D structure conductive polymer coating and organic conjugated carbonyl compounds introduce an innovative approach to the development of promising cathode materials for ASSLIBs, granting the higher specific charge, stable and reversible capacity and good reversibility even at high rate cycles.

3.1.2. Anode

With the ever-increasing energy storages demands for various technological applications, graphite, the traditional graphite-based anode materials in lithium ion batteries does not meet with high energy needs due to its limited theoretical specific capacity of $\sim 370 \text{ mAh g}^{-1}$ [153,154]. The solid-state electrolyte makes it possible for the use of metallic lithium anodes that has a low redox potential of -3.04 V vs. standard hydrogen electrode and a high specific capacity of 3860 mAh

g^{-1} , which is over 10 times that of graphite have been intensively investigated for applications as advanced energy storage materials in recent years [155,156]. Although they possess these advantages, ASSLIBs adopted lithium metal anode still suffered from serious challenges including uncontrolled growth of dendritic and mossy Li on its surface, as well as coulombic efficiency, have greatly impeded the industrial production of Li metal as anodes over past few decades. Due to the extremely low electrochemical potential of Li^+/Li , Li can spontaneously react with most organic electrolytes and Li salts to ultimately form solid electrolyte interface (SEI) layers on the anode surface. As a hostless electrode, an inevitable formation of fissures will occur on the natural SEI layers due to the constant Li stripping/plating process. Subsequently, the local concentration of Li^+ increase because of the exposed fresh Li in the cracks, resulting in the growth of undesirable lithium dendrites and induce a new SEI layer construction. This infinite consumption of the electrolyte and the accumulation of dead Li caused by the repeated breakage and regenerative SEI layers could be the fundamental response for the low coulombic efficiency and short lifespan of ASSLIBs [157–159]. Moreover, the uneven current distribution tends to accelerate the growth of the spinous Li dendrites, which could pierce the separator and give rise to an internal short circuit, thus leading to a serious hazard [156]. These two mainly problems will also mutually affect each other and consume the electrolyte irreversibly due to the high reactivity of lithium metal. As a net result of all the above situations, the electrochemical performance of LIBs fades sharply during cycling

3.1.2.1. Lithium metal anode. To overcome the above-mentioned issues, considerable effort has been devoted to regulating the growth of dendritic Li and stabilizing the formation of the SEI layer by adding electrolyte additives, solid state electrolyte, artificial SEIs and lithiophilic anodic hosts. These strategies aim at stopping the dendrite nucleation at the dendrite formation stage and/or preventing its penetration at the dendrite growth stage. Various electrolyte additives, such as vinylene carbonate (VC) [160], fluoroethylene carbonate (FEC) [161], hydrofluoric acid (HF) [162], Li nitrate (LiNO_3) [163], halogenated Li (LiF) [164], Li polysulfide (Li_2S_x) [165], and cesium ions (Cs^+) [166], have been introduced into the electrolyte to form a stable SEI layer on the Li surface and reduce the aggressive reactions between the interfaces, ultimately restraining the Li dendrites sustaining growth. Due to the unsatisfactory mechanical strength and discontinuous surface structure, the protective layer cannot withstand the huge volume change during the consecutive Li plating/stripping processes. Instead of enhancing the stability of the natural SEI layer, artificial interface engineering is employed, including the introduction of LiF layers [167], interconnected hollow carbon spheres [168], and flexible Ti_3C_2 MXene (graphene, BN)-metallic Li films [169], to address the inherent issues and improve the cycling stability of Li metal anodes.

3D scaffold/lithium metal composite anode is regarded as another viable alternatives to 2D lithium metal anode because they can simultaneously lower the local current density as well as undermine the volume expansion. It was proved that the volume change and dendrite formation can be significantly reduced via the introduce of layered Li-reduced graphene oxide 3D composite anode [170–173]. Several studies with a 3D composite Li metal anode such as 3D porous Carbon/Li metal, Li-coated 3D polymer matrix presented consistent evidence. An ideal scaffold for Li encapsulation should possess the following characteristics: (i) mechanical and thermal stability toward electrochemical cycling; (ii) low gravimetric density to achieve high-energy density for the composite anode; (iii) good electrical and ionic conductivity to provide unblocked electron/ion pathway, enabling fast electron/ion transport; and (iv) relatively large surface area for Li deposition, lowering the effective electrode current density and the possibility of dendrite formation. In view of these requirement, Liang and his coworkers [160] selected the porous carbon scaffold prepared from the

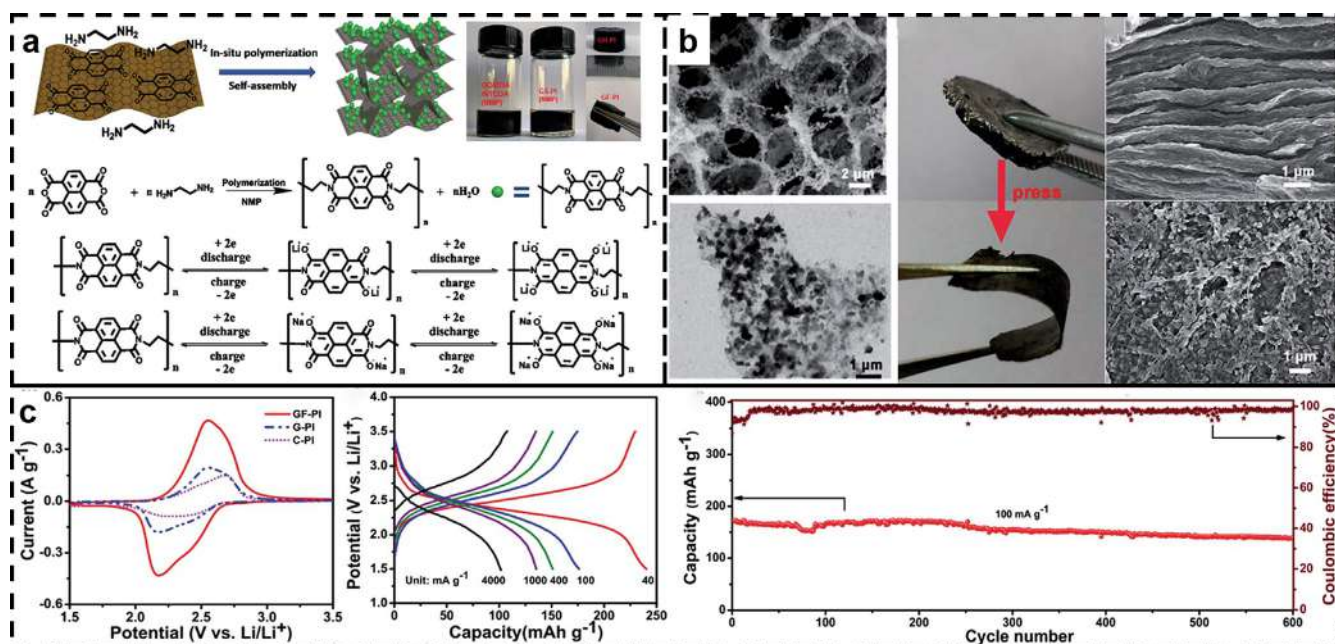


Fig. 8. (a) Schematic of the preparation process of GF-PI and electrochemical redox mechanism of PI for LIBs. (b) SEM and TEM morphology of GF-PI and a flexible binder-free GF-PI electrode. (c) Electrochemical characterization of GF-PI as a LIB cathode. Reprinted with permission [16]. Copyright 2017, Royal Society of Chemistry.

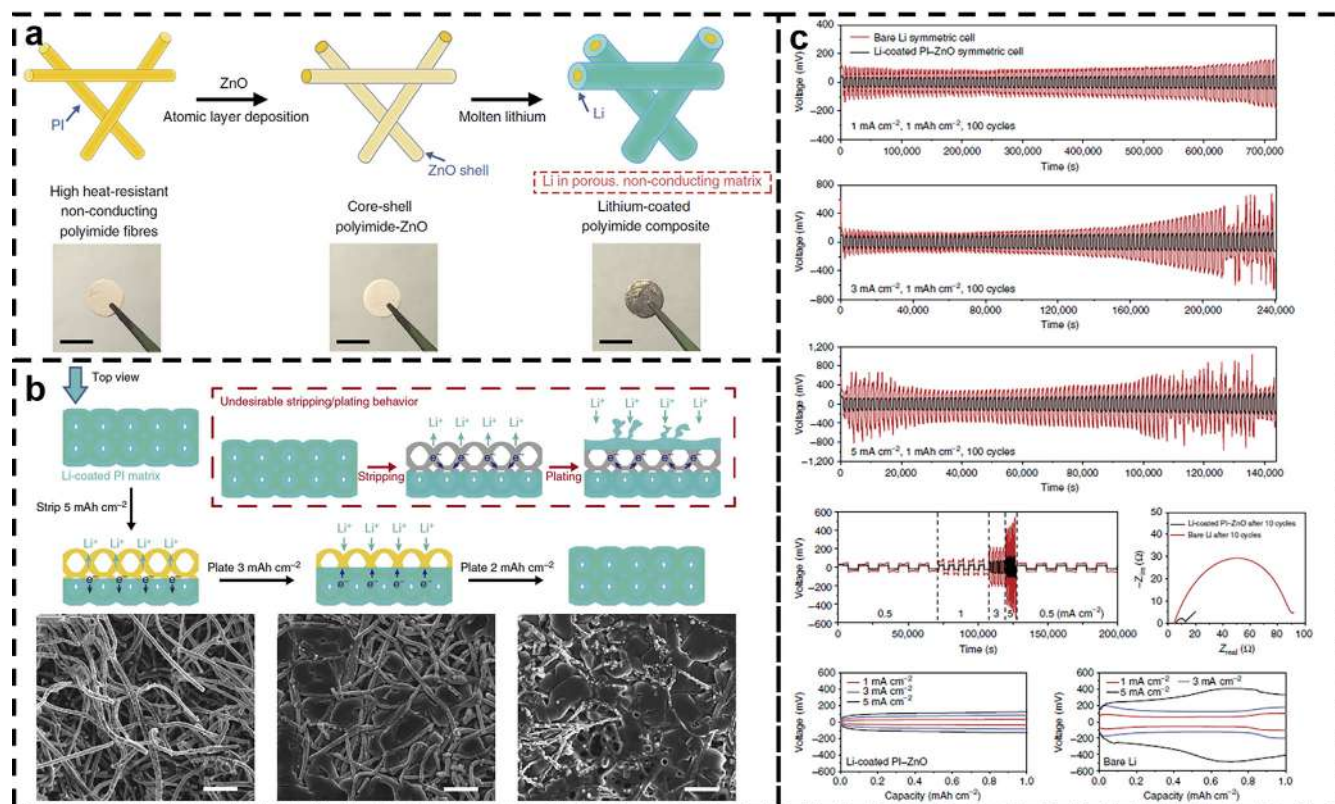


Fig. 9. (a). Schematic of the fabrication of the Li-coated PI matrix. Electrospun PI was coated with a layer of ZnO via ALD to form core-shell PI-ZnO, and the existence of ZnO coating renders the matrix 'lithiophilic' such that molten Li can steadily infuse into the matrix. (b). SEM images of Li-coated PI electrode and the alternative undesirable Li stripping/plating behavior where Li nucleate on the top surface after stripping leading to volume change and dendrites shooting out of the matrix. (c). Electrochemical characterization in EC/DEC electrolyte. Reprinted with permission [17]. Copyright 2016, Nature Publishing Group.

polyacrylonitrile (PAN) fiber, chemical vapor deposition coated Si and molten-casting lithium to fabricate a 3D framework. The volume variation and potential safety hazard was remarkably accommodated by this 3D composite anode with stable cycling over 2000 mAh g⁻¹

for > 80 cycles under 3 mA cm⁻¹. A new strategy was put forward to fabricate a free-standing polyimide (PI) matrix design for metallic Li anode [17] (Fig. 9). The electrospun polymeric fibers guarantee a chemically and electrochemically inert matrix, which is favorable to

confine the stripping/plating of Li solely within the matrix. The poor wettability between Li and PI was addressed by the adoption of ZnO that molten Li can react with ZnO and subsequently infuse into the PI matrix. This porous electrode reduces the effective current density and exhibits excellent stability for 100 cycles at 5 mA cm^{-2} . It was proved that the Li^+ can be effectively dispersed on the anode surface due to the infinity of polar groups on polymer chains like PMF, PMMA [131], thus achieve uniform Li deposition. Very recently, a 3D continuous sponge-like lithium structure with dendrite-proof blunt surface at the absence of insert host via in-situ deposition was reported by Guo et al. [132]. The electrochemical active polymer-PMMA was introduced into the interface between lithium anode and electrolyte to manipulate the Li^+ deposition behavior, in which the PMMA could react with the Li^+ and limit their unsatisfactory movement. These pre-trapped Li^+ were then in-situ reduced into initial lithium seeds to guide sequential lithium deposition at the vicinity, ending up with a morphology modeled after the 3D PMMA chains. Such 3D structure not only provided 3D continuous pathways for fast electron transport to eliminate dead Li formation without the help of foreign host but also reduced the current density over anode surface. The LIBs equipped with this 3D sponge-like anode present great enhanced rate (70 mAh g^{-1} at 2 C) and cycling performance (remained 87.6 mAh g^{-1} after 200 cycles at 1 C).

Recently, some researchers have turned their attention to the design of current collectors, as a vital ingredient of Li metal anodes, which have a remarkable influence on the formation of Li dendrites and the nucleation of Li deposition during the inception phase. It is well known that the growth of dendritic Li is attributed to the non-uniform distribution of spatial charge over the entire electrode surface [174–177]. Consequently, a homogeneous distribution of Li ion flux on the surface of a copper (Cu) substrate is urgently needed, as it plays a significant role in suppressing the growth of Li dendrites from the source. From this point of view, Lu et al. [178] proposed a free-standing Cu nanowire (CuNW) network current collector with a porous nanostructure, that encourages the plated Li metal to fill the pores and limits the formation of dendritic Li, thus the cycling stability towards lithium tremendously improved for 200 cycles with a low and stable voltage hysteresis of $\sim 0.04 \text{ V}$. In addition, it was proved that the polar surface functional groups on polymer fibers can serve as the adhesion to bind with Li^+ , promoting the Li^+ inset uniformly on the surface of anode and polymer layer [179]. The polar groups of polymer nanofibers can also provide an excellent wettability toward solid-state electrolyte. These studies reveal that the growth of dendritic lithium can be suppressed via an ingenious structure design of anode current collectors.

3.1.2.2. Other anode. Expect lithium metal anode, other metal anode also show great potential for the Li-ion batteries, such as silicon (Si) and nickel due to their high theoretical gravimetric capacity (4200 mAh g^{-1} , 1000 mAh g^{-1}), relatively low discharge potential ($0.5 \text{ V vs. Li}^+/\text{Li}$), the natural abundance of elemental and safety and environmental benignity [180,181]. However, they still suffer from poor cycling stability due to large volume expansions and contractions during Li^+ intercalation/de-intercalation. Therefore, inspired from the Li anode, many efforts have been devoted to preparing composite 3D polymer anode via combining their individual advantages. As a representative example, Wu et al. [182] reported an in-situ polymerized hydrogel composite Si-based anodes with a well-connected 3D network structure consisting of Si nanoparticles and conducting polymer. An extremely long cycling life (5000 cycles) with over 90% capacity retention at high current density (6 A g^{-1}) was demonstrated. The phosphoric acid groups in the phytic acid molecules can potentially bind with the SiO_2 on the Si particle surfaces via hydrogen bonding during polymerization, which was regarded as the main reason for the improved cycle lifetime. This interaction can also result in the conformal coating of phytic acid molecules on the surface, which may further crosslink with aniline monomers during polymerization to generate a conformal conductive coating. Additionally, the negatively charged surface oxide may

electrostatically interact with the positively charged PANi doped by the phytic acid.

The utilization of a polymer matrix with a 3D network structure provides a new horizon for the design of the state-of-the-art anode and accelerates the industrialization lithium metal and other metallic anode towards next generation high energy density battery systems.

3.1.3. Binder

Despite the cathode and anode play a critical role in the development of LIBs with high energy and power density, the ideal LIBs auxiliary materials are still indispensable, such as the binder. The binder in an electrode can connect the electrode active materials with current collector. During the charge/discharge process of LIBs, the ineluctable volume expansion and contraction is caused by the Li^+ ion intercalation and deintercalation on the electrode. As this process continues, the interface connection between active materials and binder will become weaken, along with the increase of the interface impedance in particles. The ohmic resistance of electrode will significantly increase, ultimately causing the deterioration of LIBs performance. In order to avoid the volume effect as far as possible, an ideal binder should be of low cost, strong adhesive property, high physical and electrochemical stability.

The conventional binder applied in LIBs are non-conductive high molecular polymer, which can generally be divided into two categories of organic-solvent based binder and aqueous binder [183]. Poly(vinylidene fluoride) (PVDF), is a kind of typical organic-solvent based binder which show strong thermoplasticity and high solubility in polar solvent. According to the theoretical calculation (molecular orbital theory), it exhibits highest oxidation potential (-14.08 eV) among all binders. In consequence, PVDF has been extensively used as the electrode binder in LIBs. However, PVDF still limited from its non-conductive nature and large volume effect during the lithiation/delithiation cycling process, as well as environmental unfriendly feature and relative high cost. Systematically researches have proved that the electrochemical performance of LIBs can be significantly improved through rational binder structure design [18,184]. Developing an effective conductive network structure with excellent adhesion is the key objective for desirable binder materials.

Very recently, an effective method water-based latex assembly technique has been shown to fabricate conducting nanocomposite with 3D hierarchical networks [185]. Inducing from this method, Ma et al. [18] prepared a 3D hierarchical walnut kernel shape conducting polymer as water soluble binder via emulsion polymerization (Fig. 10a). This unique 3D polymer network promoted multi-dimensional contacts with the active materials and conducting agents through non-covalent or covalent interactions. The LiFePO_4 cathode with this kind of binder showed outstanding rate performance (105 mAh g^{-1} at 5 C) compared to the traditional PVDF binder (90 mAh g^{-1} at 5 C).

Although a notable improvement of electrochemical performance has been accomplished, the conductivity of the polymer binders is still restricted by the insulating polymer chains which could severely impede the electron transportation. In Si composite anode, the Si powder and carbon particles are dispersed to acquire large contact area between two components. Upon charging, Si reacts with Li^+ and electrons with an intrinsic volume expansion, which allows a better contact between Si and carbon particles. Due to this volume expansion, the resistance would drop in the initial step. Once the dealloying occurs, however, Si particles would contract, causing poor contact with carbon and eventually the isolation of the particles from the electronic path made between current collector to carbon particles as the whole electrodes layer is not elastic enough. The loss of electronic path brings about an increase in both the contact (ohmic) resistance and charge transfer resistance for dealloying reaction. In the end, due to the huge internal resistance, the electrode potential reaches earlier at the discharging cutoff limit. In our review, the 3D structured binder could be used in hollow nanostructures to cause desirable volume expansion

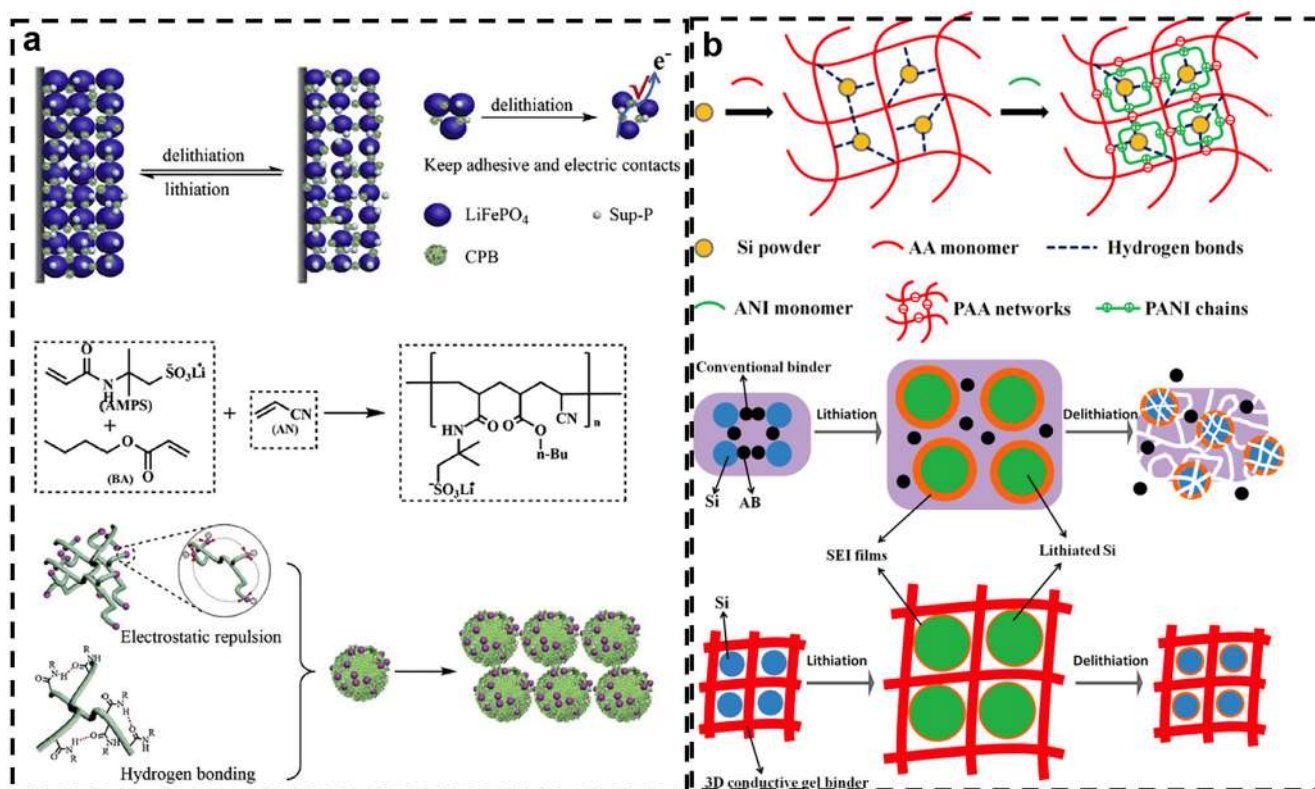


Fig. 10. (a). Schematic illustration of the synthesis and proposed mechanism of the conductive polymer binder (CPB), Replacing one-dimensional binder or two-dimensional binder, 3D conductive binder could keep the electrical and mechanical integrity of the electrode during charge/discharge cycles. (b). The formation process of the 3D conductive PAA/PANI IPN binder for Si anodes and the process of Li^+ insertion and extraction using different binders. Reprinted with permission [18,184].

away from the outer surface so that the increase in outer surface area during reaction could be minimized and allow for the formation of stable SEI layer, which is critical for the lower resistance [186]. To form efficient conducting route between the active materials and reduce the volume expansion, the most meaningful method is introducing a conductive polymer into common polymer-based binder, which could not only eliminate the utilization of conductive additives and increase the energy density, but also keep the balance of electrical conductivity and structure stability of the electrode. In this case, Yu et al. [184], developed a 3D conductive interpenetrated gel network as a promising binder for high performance Si anode via a facile in situ polymerization route of aniline into the PAA hydrogel network (Fig. 10b). This 3D gel polymer binder could not only accommodate the volume expansion and maintain electric connectivity, but also assist in the formation of stable solid electrolyte interphase (SEI) membranes. This Si anode with PAA/PANI IPN binder exhibited a high capacity of 2205 mAh g^{-1} after 300 cycles with a high Coulombic efficiency above 99%.

It is believed that a well-designed 3D polymer-based binder has a great potential to be applied for both cathode and anode with great volume expansion, to improve the electrochemical performance of ASSLIBs during high rate charging/discharging and long-term cycling process.

3.2. 3D polymer composite electrolyte for ASSLIBs

The safety issues haunting over commercial LIBs can be addressed through replacing liquid electrolyte with the solid-state electrolyte. Developing suitable solid-state electrolyte for high energy density of ASSLIBs is critical yet challenge [13]. The solid-state electrolyte can be generally divided into two classes of materials: solid polymer electrolyte (SPE) and inorganic ceramic electrolyte. Although inorganic ceramic electrolyte is rigid and nonflammable, which is generally

considered as the ultimate solution for the ASSLIBs. However, utilizing inorganic ceramic electrolyte struggled in low ionic conductivity and high interfacial resistance to electrodes (both cathode and anode) [187]. In addition, several ceramic solid electrolytes have been extensively investigated to date. It is confirmed that they are easily reduced by Li metal and they have failed to block dendrite formation as well as the growth between their grain boundaries [188]. While solid polymer electrolytes (SPEs) have been also widely investigated due to their excellent flexibility, easy processing and good interface contact with electrodes. The ion transport mechanism in SPEs is normally regarded that the polar groups on polymer chains can coordinate with the Li^+ via the interaction and the polymer owns the chain flexibility to promote the ion hopping. Ion transport is assisted by the segmental motion of polymer chains and thus the amorphous of polymer is the preferable region. Under an electrical field, long distance transport is realized by continuous hopping, and the number of free ions depends on the dissociation ability of the lithium salt in the polymer [13]. Taking consideration of these characteristics, 3D polymeric electrolytes of ASSLIBs must exhibit the following properties: (i) high room temperature ionic conductivity; (ii) low electronic conductivity; (iii) sufficient mechanical strength to inhibit lithium dendrites; (iv) good electrochemical stability window toward lithium metal; and (v) excellent compatibility with other additives.

To enhance the kinetics of amorphous fraction towards SPEs at room temperature (RT), composite polymer electrolytes (CPEs) developed by the integration of non- Li^+ -conductive (such as SiO_2 and TiO_2) [189,190] or Li^+ -conductive (such as perovskite-type $\text{Li}_{0.3}\text{La}_{0.557}\text{TiO}_3$ (LLTO), and garnet-type $\text{Li}_7\text{La}_3\text{Zr}_2\text{O}_{12}$ (LLZO)) [191,192] fillers into the polymer matrix or crosslinking, copolymerization methods are proven to be effective strategies. For example, Cui et al adopted an in-situ hydrolysis methods to acquire zero-dimensional (0D) SiO_2 nanoparticles and homodisperse in the PEO matrix to obtain CPEs [190].

The crystallinity of PEO was effectively decreased and ultimately achieving an ionic conductivity of $4.4 \times 10^{-5} \text{ S cm}^{-1}$ at 30°C . Subsequently, they conformed one-dimensional (1D) polyacrylonitrile (PAN)-based CPEs exhibits several orders of magnitude of ionic conductivity than that of 0D LLTO fillers [193]. One-dimensional nanofibers can not only reduce the crystallinity of PEO or PAN matrix but also serve as ion conducting pathways because of their large length-to-diameter ratio [194]. Although the ionic conductivity of CPEs has improved somewhat through the above-mentioned strategies, it still has room to improve the performance of the CPEs, especially the 3D structure among the CPEs. In this part, we will discuss the recent achievement of composite 3D polymer including organic/organic composite and organic/inorganic composite applied in solid-state electrolyte.

3.2.1. Organic/organic composite 3D electrolyte

Over the years, extensive efforts have been made to improve the performance of the CPEs through the organic/organic composite 3D structures. Among these, gel polymer electrolyte (GPE) composite with multifunctional polymer to form rigid-flexible cross-linked network is considered as a novel strategy to realize relatively higher ionic conductivity and form stabilized SEI layer for ASSLIBs. For example, a dual-salt (LiTFSI-LiPF_6) CPE with 3D cross-linked polymer networks was designed to inhibit the lithium dendrite growth and build stable SEI layers [21]. This cross-linked 3D polymerized by poly (ethylene glycol) diacrylate (PEGDA) and ethoxylated trimethylolpropane triacrylate (ETPTA) was prepared simultaneously introducing dual-salt electrolyte in the 3D structure (Fig. 11a). Multiple reaction sites of PEGDA and ETPTA provided possibilities of polymerizing reactions under thermal initiation, then the 3D network structure formed via auto-polymerization as well as copolymerization. As a result, the thermostabilization and ion transference of CPEs were enhanced [195,196]. The functional monomers are applied in work function as follows: the linear molecular chains of PEGDA greatly benefits the lithium ions transference, while triple branches of ETPTA largely acting as a cross-linking structure and forming networks. Consequently, the CPEs basically solved the existing

intractable issues of LIBs, ensuring an enhanced ionic conductivity (0.56 mS cm^{-1} at room temperature) and blocking lithium dendrite effective (87.93% capacity retention after 300 cycles). Compared to the traditional irregular lithium deposition of liquid electrolyte, the tight compact of CPEs ensured uniform Li^+ distribution and lithium deposition.

Generally, the incorporation of a chemically cross-linked structure permeating the host polymer is regarded as an effective method for improving the mechanical properties and the thermal/dimensional stability of CPEs. However, the currently used cross-linking reactions are usually initiated by thermal radicals such as benzoyl peroxide, di(4-t-butylcyclohexyl) peroxy carbonate, and azobisisobutyronitrile. These radical initiation processes have an inherent disadvantage in that the by-products of the thermal initiators such as free radicals and residual monomer are highly reactive with Li metal. These reaction products cover the surface of the Li metal, increasing the electrode resistance and severely degrading the battery performance. Thus, epoxy ring-opening polymerization has been applied in the production of high-purity polymer membranes with wide applications as industrial binders and surfacing coatings [199,200], and this process under mild conditions totally free of thermal initiators and without the formation of small molecule by-products. It is potential that such a process is ideal for producing a CPE meeting the following requirement: simple preparation, high mechanical strength, high ionic conductivity, excellent thermal and dimensional stability, and more importantly, free of by-products formation through a thermal initiator. On this basis, Lu and his co-workers [197,198] reported a novel initiator-free one-pot synthesis strategy based on a ring-opening polymerization reaction to prepare a tough and compact 3D network gel polymer electrolyte (3D-GPE) (Fig. 11b). In the production process, diglycidyl ether of bisphenol-A (DEBA) is used as the supporting framework to enhance the mechanical strength of the polymer matrix, while poly (ethylene glycol) diglycidyl ether (PEGDE) and diamino-poly (propylene oxide) (DPPO) are cross-linked throughout this framework to guarantee fast ion transference. The linear poly (vinylidene fluoride-co-hexafluoropropylene) (denoted PVDF-HFP) chain embedded in the polymeric network provided the

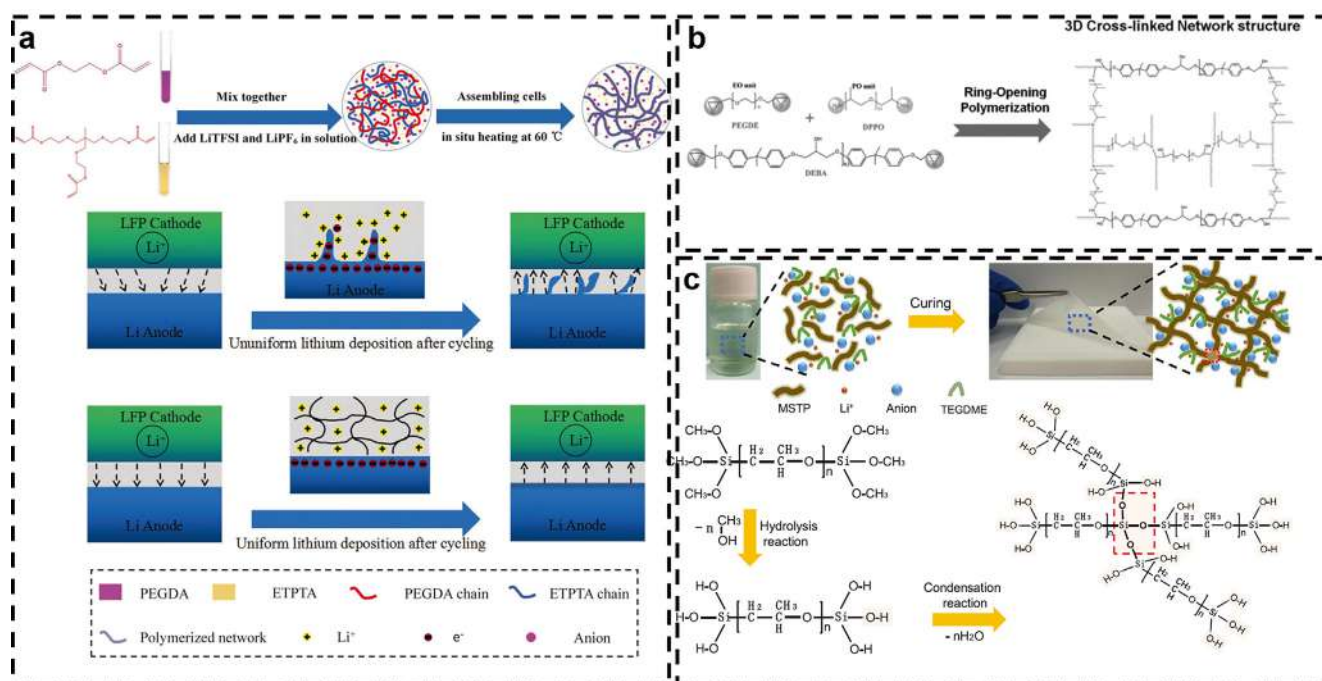


Fig. 11. (a) The specific synthesis route for in situ polymerization of dual-salt 3D-crosslinked CPEs and the changes in the Li electrodes with 3D-CPE during the Li plating/stripping [21]. (b) Synthesis of the 3D-GPE membrane [197]. (c) The molecular structures of the MSTP monomer and the MSTP-PE with the polymerization process. The chemical bonds in the light red area are the cross-linking parts [19]. Reprinted with permission [19,21,198]. (For interpretation of the references to colour in this figure legend, the reader is referred to the web version of this article.)

membrane excellent flexibility. In addition, the contact between electrolyte and lithium metal was reduced by incorporating the carbonate solvent molecules in the 3D-GPE polymeric framework and significantly suppressed the formation of a thick SEI layer, which contributed to an even distribution of the Li^+ flux.

3.2.2. Organic/inorganic composite 3D electrolyte

SPEs composite with active inorganic fillers have been demonstrated to be an effective strategy to enhance the performance of ASSLIBs. The drawbacks of inorganic electrolytes on flexibility and interfacial wetting property can be exhibited in the solid composite electrolyte. For example, the lithium aluminum titanium phosphate (LATP) with the sodium superionic conductor (NASICON)-type structure has been widely investigated as a competitive Li^+ conductor because of its high ionic conductivity ($> 10^{-3} \text{ S cm}^{-1}$), good stability at room temperature, and simple integrability. However, when LATP directly contact with lithium metal, it exhibits a chemical instability because of the reduction of Ti^{4+} . Typically, $\text{Li}_{1.4}\text{Al}_{0.4}\text{Ti}_{1.6}(\text{PO}_4)_3$ (LATP) was used as fillers to prepare CPEs (PEO-LATP) and the particle-fillers composite PEO-LATP was demonstrated with unsatisfactory electrochemical stability in Li metal batteries, which indicated that LATP probably reacted with Li metal when directly mixed with PEO as particle-fillers [201,202]. To improve stability and maintaining ionic conductivity, a 3D fiber-network-reinforced bicontinuous CPEs with high stability and Li dendrites suppression against Li metal for ASSLIBs. LATP composite with polyacrylonitrile (PAN) as a network filler prepared by electrospinning promoted to improve the mechanical property of PEO-based polymer matrix and enhance ionic conductivities by decreased segmental reorientations of polymers. Meanwhile, the reaction of LATP with Li anode was effectively inhibited from utterly isolating chemically active Ti^{4+} with Li metal because LATP particles are well-enveloped within PAN polymeric chains. Thus, a high ionic conductivity ($\sim 10^{-4} \text{ S cm}^{-1}$) and extended electrochemical window ($> 5 \text{ V}$) were acquired [202].

The improved performance of inorganic/organic CPEs are attributed to the rapid interphase conduction between active filler and polymer electrolyte [193,203]. For this reason, the conductivity improves as the filler ratio increases owing to the higher interphase volume. However, after reaching a certain filler ratio, the conductivity begins to decrease as a result of the particle agglomeration at high concentration which lowers the volume fraction of interphase and destroys the percolated network of interphase [202,204]. In this circumstance, nanostructured fillers were adopted to address this problem, which can lower percolation threshold through the high specific aspect ratio, and superior Li^+ conductivity compared to the pristine inorganic fillers. It is particularly important to form a percolated network of nanofillers with high filler concentration to take full advantage of rapid conduction along the interface. Moreover, a higher ratio of nanofillers will also lead to a relatively low weight ratio of polymer, which is essential for the improvement of the electrochemical stability and battery safety [205,206]. Among several approaches, the 3D nanostructured hydrogel frameworks have been widely developed to provide various merits such as tunable hierarchical structures and 3D channels for facilitated ion/electron transport. Recently, a 3D nanostructured hydrogel derived pre-percolated $\text{Li}_{0.35}\text{La}_{0.55}\text{TiO}_3$ (LLTO) frameworks for high-performance CPEs was proposed [20]. (Fig. 12) After a simple gelation of the precursors and hydrogel, a continuous framework was formed via the heat treatment. This interconnected 3D percolating nanostructure consisted of nanoscale phase separation of polymer, water and LLTO. This CPE with LLTO framework exhibited a high ceramic content (44 wt%) and an improved ionic conductivity of $1.5 \times 10^{-4} \text{ S cm}^{-1}$ at room temperature. The PVA in this system would stem the segmental motion of polymer chains and lower the activation energies ($E_a = 0.64 \text{ eV}$) above the melting temperature [207], which was critical factor for fast Li^+ transport. In addition, the pre-percolated LLTO network could provide a continuous interphase as a pathway for Li^+ conduction, as well as

providing a 3D interconnected structure.

4. 3D polymers for other batteries

There is more and more research employed 3D conductive network for Li-S batteries [141,208], Na-ion batteries [129], Li-O₂ batteries [209]. As similar to the commercial LIBs, the development of other batteries based on inorganic materials are also limited by slow ionic diffusion rates, low theoretical capacity and structural instability. Inspired by the application in LIBs, the 3D polymer binder has been extensively utilized in electrode to replace conventional PVDF binder because of their high ionic conductivity and stability. Recently, a 3D cross-linked polyethylene oxide (PEO)/tannic acid (TA) binder have exhibited excellent adhesiveness and multiple functions [143]. As a kind of plant polyphenols, TA can cross-link with the water-soluble polymer like PEO via hydrogen bond and reduce the solubility of polymers [210]. A 3D cross-linked network is built up due to these abundant hydroxyl and ether groups between PEO and TA chains. This unique 3D PEO/TA would maintain cathode integrity and benefit the corresponding cathode to buffer the volume change. Additionally, the strong interaction in TA can chemically anchor polysulfides through the dipole-dipole interaction to retard the shuttling effect. This multifunctional 3D binder provides a simple and effective strategy for the construction of excellent performance cathodes towards Li-S batteries, which also applies to advanced ASSLIBs, Li-O₂ batteries and Na-ion batteries.

5. Summary and outlook

In this review, we have discussed recent advances on the synthetic strategies and solid-state electrochemical energy storage applications of 3D polymers. In summary, 3D polymers can be rationally constructed via inclusion polymers with existing 3D frameworks, adding cross-linkers into polymers or self-crosslinking polymer chains. Due to the unique interconnected networks and highly continuous porous structure of 3D polymers, it can be widely employed to fabricate high performance solid-state electrochemical energy storage devices including SSCs and ASSLIBs. It can be clearly concluded that electrochemical performance of energy storage devices is closely related to the synthetic routes of 3D polymers, nanostructures and pore size of 3D polymers, interfacial interaction between 3D polymers and other functional components. Beyond the exciting advances reported in state-of-the-art works summarized by this review, we believe that there are considerable opportunities and challenges remaining for further investigation.

One for the supercapacitor, (i) *Cyclic stability of SSCs 3D polymer electrodes*. Although 3D polymers with high electrochemical activity are demonstrated to be beneficial to increasing specific capacitance and energy density of SSCs electrodes, they still suffer from poor cyclic stability due to limited electronic conductivity. Moreover, the doping and de-doping process of CPs usually leads to structure collapse of 3D polymeric networks, which will also deteriorate cyclic stability of SSCs. Inclusion 3D polymers with carbonaceous materials is demonstrated to enhance cyclic stability and conductivity of 3D polymers simultaneously, but it is challenging to obtain considerable carbon/CPs interfaces. In this content, future works should shed light on increasing cyclic stability of 3D polymer SSCs electrodes and understanding interfacial interactions between CPs and carbonaceous materials. (ii) *Ionic conductivity and interface of SSCs 3D polymer electrolyte*. One of the biggest challenges of solid-state 3D polymer electrolyte is increasing its ionic conductivity. Modifications to the electrolyte film in order to improve its water retention capability and to reduce the sensitivity to the environment are essential. Due to the fact that few studies are devoted to the electrode-electrolyte interfaces, starting from the gel form to the solidified form of the electrolyte. More fundamental work is needed to fully understand the ion transport in SSCs electrolyte and their interaction with electrode materials to maximize ion mobility

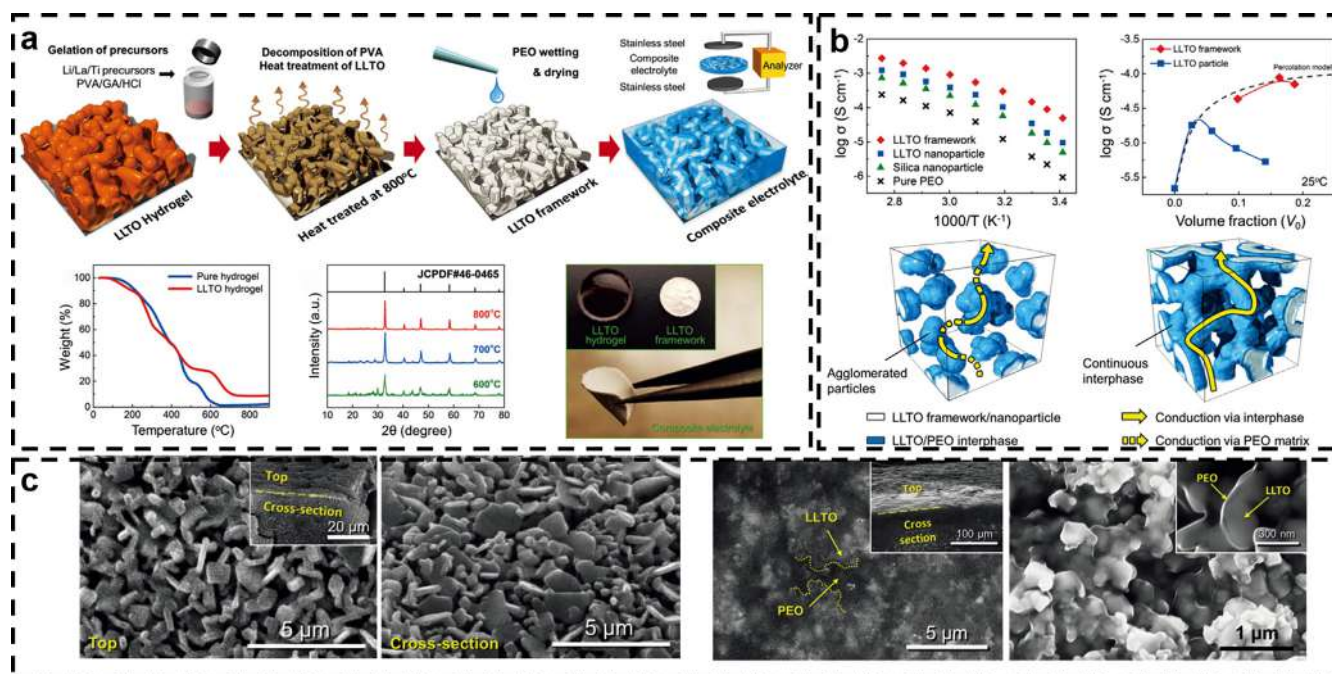


Fig. 12. (a). Schematic representation of LLTO framework composite electrolyte and the thermogravimetric analysis, XRD patterns and photographs of composite electrolytes. (b). Ionic conductivity of LLTO framework and conductive mechanism in composite electrolyte with agglomerated nanoparticles and 3D porous framework. (c). The surface and cross-section morphology of LLTO frameworks and composite electrolyte. Reprinted with permission [20].

while minimizing self-discharge.

As for the ASSLIBs, First, it should be noted that the electrochemical properties of each component are critical for the development of high-performance 3D polymer based ASSLIBs. For electrodes, several novel organic electrodes or conductive polymers available to be integrated to acquire superior 3D structure and excellent electrochemical performance and robust cycling stability. Meanwhile, more electrode materials need to be tested with solid-state electrolyte, which is essential for the development of ASSLIBs. In terms of the electrolyte, further optimization is required. The development of 3D structural solid-state electrolyte with higher ionic conductivity and larger electrochemical stability windows is a significant trend in the future. Second, non-uniformity of the polymer matrix in terms of size, shape, and functional groups existed on the polymer surface inhibited the precisely-controlled reaction/fabrication and deep understanding of the assembly mechanism during polymer-based 3D network architectures. It is essential to develop a proper strategy to avoid the intrinsic polymer thermodynamic instabilities during the assembly 3D structure process and facile preparation to acquire high quality materials with these unique structure on large scale. Third, the electrode/electrolyte interface is a problem of great importance for cycling stability of ASSLIBs. In spite of the lithium dendrites growth and SEI layers deteriorate can be partially inhibited via the 3D polymer structure, precise characterizations like in-situ analysis are required to facilitate the understanding of the significance of this architecture and ultimately achieving dendrite-free and dense stable SEI layer in practical applications. Further, it is an urgent need to develop some easy, fast and controlled manufacturing processes for 3D polymer materials in order to achieve large-scale and low-cost production.

Looking to the future, energy storage technologies will continue to increase due to the fact that the demand for renewable energy sources is increasing in soaring rate, but scale-up and commercialization of 3D polymer based solid-state electrochemical energy storage devices still need to overcome many hurdles. Therefore, comprehensive approaches and multi-disciplinary efforts is necessary to push the research frontiers forward. As evidenced in this review, these 3D polymer and 3D polymer-based composites enabled high performance solid-state

electrochemical energy storage technology and device will become mature in the near future.

Declaration of Competing Interest

The authors declare that they have no known competing financial interests or personal relationships that could have appeared to influence the work reported in this paper.

Acknowledgments

This work is supported the National Natural Science Foundation of China (No. 51977185 and No. 51972277) and Sichuan Science and Technology Program (No. 2018RZ0074).

References

- [1] J.P. Holdren, Energy and sustainability, *Science* 315 (5813) (2007) 737, <https://doi.org/10.1126/science.1139792>.
- [2] T. Elmqvist, E. Andersson, N. Frantzeskaki, T. McPhearson, P. Olsson, O. Gaffney, K. Takeuchi, C. Folke, Sustainability and resilience for transformation in the urban century, *Nat. Sustain.* 2 (4) (2019) 267–273, <https://doi.org/10.1038/s41893-019-0250-1>.
- [3] Z.L. Wang, T. Jiang, L. Xu, Toward the blue energy dream by triboelectric nanogenerator networks, *Nano Energy* 39 (2017) 9–23, <https://doi.org/10.1016/j.nanoen.2017.06.035>.
- [4] D.M. Kammen, D.A. Sunter, City-integrated renewable energy for urban sustainability, *Science* 352 (6288) (2016) 922–928, <https://doi.org/10.1126/science.aad9302>.
- [5] K. Shen, J. Ding, S. Yang, 3D Printing Quasi-Solid-State Asymmetric Micro-Supercapacitors with Ultrahigh Areal Energy Density, *Adv. Energy Mater.* 8 (20) (2018) 1800408, <https://doi.org/10.1002/aenm.201800408>.
- [6] D.P. Dubal, N.R. Chodankar, D.H. Kim, P. Gomez-Romero, Towards flexible solid-state supercapacitors for smart and wearable electronics, *Chem. Soc. Rev.* 47 (6) (2018) 2065–2129, <https://doi.org/10.1039/c7cs00505a>.
- [7] X. Lu, M. Yu, G. Wang, Y. Tong, Y. Li, Flexible solid-state supercapacitors: design, fabrication and applications, *Energy Environ. Sci.* 7 (7) (2014) 2160–2181, <https://doi.org/10.1039/c4ee00960f>.
- [8] P. Yang, W. Mai, Flexible solid-state electrochemical supercapacitors, *Nano Energy* 8 (2014) 274–290, <https://doi.org/10.1016/j.nanoen.2014.05.022>.
- [9] A. Eftekhari, L. Li, Y. Yang, Polyaniline supercapacitors, *J. Power Sources* 347 (2017) 86–107, <https://doi.org/10.1016/j.jpowsour.2017.02.054>.
- [10] J. Banerjee, K. Dutta, M.A. Kader, S.K. Nayak, An overview on the recent

- developments in polyaniline-based supercapacitors, *Polym. Adv. Technol.* 30 (8) (2019) 1902–1921, <https://doi.org/10.1002/pat.4624>.
- [11] L. Hao, X. Li, L. Zhi, Carbonaceous electrode materials for supercapacitors, *Adv. Mater.* 25 (28) (2013) 3899–3904, <https://doi.org/10.1002/adma.201301204>.
- [12] Z. Lin, E. Goikolea, A. Balducci, K. Naoui, P.L. Taberna, M. Salanne, G. Yushin, P. Simon, Materials for supercapacitors: when Li-ion battery power is not enough, *Mater. Today* 21 (4) (2018) 419–436, <https://doi.org/10.1016/j.mattod.2018.01.035>.
- [13] A. Manthiram, X. Yu, S. Wang, Lithium battery chemistries enabled by solid-state electrolytes, *Nat. Rev. Mater.* 2 (4) (2017) 16103, <https://doi.org/10.1038/natrevmats.2016.103>.
- [14] F. Bu, I. Shakir, Y. Xu, 3D Graphene Composites for Efficient Electrochemical Energy Storage, *Adv. Mater. Interfaces* 5 (15) (2018) 1800468, <https://doi.org/10.1002/admi.201800468>.
- [15] M. Wang, X. Duan, Y. Xu, X. Duan, Functional three-dimensional graphene/polymer composites, *ACS Nano* 10 (8) (2016) 7231–7247, <https://doi.org/10.1021/acsnano.6b03349>.
- [16] Y. Huang, K. Li, J. Liu, X. Zhong, X. Duan, I. Shakir, Y. Xu, Three-dimensional graphene/polyimide composite-derived flexible high-performance organic cathode for rechargeable lithium and sodium batteries, *J. Mater. Chem. A* 5 (6) (2017) 2710–2716, <https://doi.org/10.1039/c6ta09754e>.
- [17] Y. Liu, D. Lin, Z. Liang, J. Zhao, K. Yan, Y. Cui, Lithium-coated polymeric matrix as a minimum volume-change and dendrite-free lithium metal anode, *Nat. Commun.* 7 (2016) 10992, <https://doi.org/10.1038/ncomms10992>.
- [18] X. Ma, S. Zou, A. Tang, L. Chen, Z. Deng, B.G. Pollet, S. Ji, Three-dimensional hierarchical walnut kernel shape conducting polymer as water soluble binder for lithium-ion battery, *Electrochim. Acta* 269 (2018) 571–579, <https://doi.org/10.1016/j.electacta.2018.03.031>.
- [19] Z. Lin, X. Guo, H. Yu, Amorphous modified silyl-terminated 3D polymer electrolyte for high-performance lithium metal battery, *Nano Energy* 41 (2017) 646–653, <https://doi.org/10.1016/j.nanoen.2017.10.021>.
- [20] J. Bae, Y. Li, J. Zhang, X. Zhou, F. Zhao, Y. Shi, J.B. Goodenough, G. Yu, A 3D Nanostructured Hydrogel-Framework-Derived High-Performance Composite Polymer Lithium-Ion Electrolyte, *Angew. Chem. Int. Edit.* 57 (8) (2018) 2096–2100, <https://doi.org/10.1002/anie.201710841>.
- [21] W. Fan, N.-W. Li, X. Zhang, S. Zhao, R. Cao, Y. Yin, Y. Xing, J. Wang, Y.-G. Guo, C. Li, A dual-salt gel polymer electrolyte with 3D cross-linked polymer network for dendrite-free lithium metal batteries, *Adv. Sci.* 5 (9) (2018) 1800559, <https://doi.org/10.1002/advs.201800559>.
- [22] Y. Ji, N. Liang, J. Xu, D. Zuo, D. Chen, H. Zhang, Cellulose and poly(vinyl alcohol) composite gels as separators for quasi-solid-state electric double layer capacitors, *Cellulose* 26 (2) (2018) 1055–1065, <https://doi.org/10.1007/s10570-018-2123-6>.
- [23] H. Yu, J. Wu, L. Fan, Y. Lin, K. Xu, Z. Tang, C. Cheng, S. Tang, J. Lin, M. Huang, Z. Lan, A novel redox-mediated gel polymer electrolyte for high-performance supercapacitor, *J. Power Sources* 198 (2012) 402–407, <https://doi.org/10.1016/j.jpowsour.2011.09.110>.
- [24] S. Pan, J. Deng, G. Guan, Y. Zhang, P. Chen, J. Ren, H. Peng, A redox-active gel electrolyte for fiber-shaped supercapacitor with high area specific capacitance, *J. Mater. Chem. A* 3 (12) (2015) 6286–6290, <https://doi.org/10.1039/c5ta00007f>.
- [25] Y. Wang, Y. Shi, L. Pan, Y. Ding, Y. Zhao, Y. Li, Y. Shi, G. Yu, Dopant-Enabled Supramolecular Approach for Controlled Synthesis of Nanostructured Conductive Polymer Hydrogels, *Nano Lett.* 15 (11) (2015) 7736–7741, <https://doi.org/10.1021/acs.nanolett.5b03891>.
- [26] X. Chu, H. Zhang, H. Su, F. Liu, B. Gu, H. Huang, H. Zhang, W. Deng, X. Zheng, W. Yang, A novel stretchable supercapacitor electrode with high linear capacitance, *Chem. Eng. J.* 349 (2018) 168–175, <https://doi.org/10.1016/j.cej.2018.05.090>.
- [27] L. Pan, G. Yu, D. Zhai, H.R. Lee, W. Zhao, N. Liu, H. Wang, B.C. Tee, Y. Shi, Y. Cui, Z. Bao, Hierarchical nanostructured conducting polymer hydrogel with high electrochemical activity, *P. Natl. Acad. Sci. USA* 109 (24) (2012) 9287–9292, <https://doi.org/10.1073/pnas.1202636109>.
- [28] P. Simon, Y. Gogotsi, Materials for electrochemical capacitors, *Nat. Mater.* 7 (11) (2008) 845–854, <https://doi.org/10.1038/nmat2297>.
- [29] B. Gu, H. Su, X. Chu, Q. Wang, H. Huang, J. He, T. Wu, W. Deng, H. Zhang, W. Yang, Rationally assembled porous carbon superstructures for advanced supercapacitors, *Chem. Eng. J.* 361 (2019) 1296–1303, <https://doi.org/10.1016/j.cej.2019.01.007>.
- [30] H. Su, H. Zhang, F. Liu, F. Chun, B. Zhang, X. Chu, H. Huang, W. Deng, B. Gu, H. Zhang, X. Zheng, M. Zhu, W. Yang, High power supercapacitors based on hierarchically porous sheet-like nanocarbons with ionic liquid electrolytes, *Chem. Eng. J.* 322 (2017) 73–81, <https://doi.org/10.1016/j.cej.2017.04.012>.
- [31] H. Zhang, X. Zhang, H. Lin, K. Wang, X. Sun, N. Xu, C. Li, Y. Ma, Graphene and maghemite composites based supercapacitors delivering high volumetric capacitance and extraordinary cycling stability, *Electrochim. Acta* 156 (2015) 70–76, <https://doi.org/10.1016/j.electacta.2015.01.041>.
- [32] Z. Wang, H. Su, F. Liu, X. Chu, C. Yan, B. Gu, H. Huang, T. Yang, N. Chen, Y. Han, W. Deng, H. Zhang, W. Yang, Establishing highly-efficient surface faradaic reaction in flower-like NiCo₂O₄ nano-/micro-structures for next-generation supercapacitors, *Electrochim. Acta* 307 (2019) 302–309, <https://doi.org/10.1016/j.electacta.2019.03.227>.
- [33] F. Liu, X. Chu, H. Zhang, B. Zhang, H. Su, L. Jin, Z. Wang, H. Huang, W. Yang, Synthesis of self-assembly 3D porous Ni(OH)₂ with high capacitance for hybrid supercapacitors, *Electrochim. Acta* 269 (2018) 102–110, <https://doi.org/10.1016/j.electacta.2018.02.130>.
- [34] A. VahidMohammadi, J. Moncada, H. Chen, E. Kayali, J. Orangi, C.A. Carrero, M. Beidaghi, Thick and freestanding MXene/PANI pseudocapacitive electrodes with ultrahigh specific capacitance, *J. Mater. Chem. A* 6 (44) (2018) 22123–22133, <https://doi.org/10.1039/c8ta05807e>.
- [35] Y. Huang, H. Li, Z. Wang, M. Zhu, Z. Pei, Q. Xue, Y. Huang, C. Zhi, Nanostructured Polypyrrole as a flexible electrode material of supercapacitor, *Nano Energy* 22 (2016) 422–438, <https://doi.org/10.1016/j.nanoen.2016.02.047>.
- [36] A. Chortos, Z. Bao, Skin-inspired electronic devices, *Mater. Today* 17 (7) (2014) 321–331, <https://doi.org/10.1016/j.mattod.2014.05.006>.
- [37] R. Wang, X. Du, J. Zhai, X. Xie, Distance and color change based hydrogel sensor for visual quantitative determination of buffer concentrations, *ACS Sensors* 4 (4) (2019) 1017–1022, <https://doi.org/10.1021/acssensors.9b00186>.
- [38] Y. Liang, X. Wang, W. An, Y. Li, J. Hu, W. Cui, Ag-C3N₄@ppy-rGO 3D structure hydrogel for efficient photocatalysis, *Appl. Surf. Sci.* 466 (2019) 666–672, <https://doi.org/10.1016/j.apsusc.2018.10.059>.
- [39] T. Thambi, Y. Li, D.S. Lee, Injectable hydrogels for sustained release of therapeutic agents, *J. Controlled Release* 267 (2017) 57–66, <https://doi.org/10.1016/j.jconrel.2017.08.006>.
- [40] R. Dimatteo, N.J. Darling, T. Segura, In situ forming injectable hydrogels for drug delivery and wound repair, *Adv. Drug Deliv. Rev.* 127 (2018) 167–184, <https://doi.org/10.1016/j.addr.2018.03.007>.
- [41] Y. Lin, H. Zhang, H. Liao, Y. Zhao, K. Li, A physically crosslinked, self-healing hydrogel electrolyte for nano-wire PANI flexible supercapacitors, *Chem. Eng. J.* 367 (2019) 139–148, <https://doi.org/10.1016/j.cej.2019.02.064>.
- [42] C. Yang, P. Zhang, A. Nautiyal, S. Li, N. Liu, J. Yin, K. Deng, X. Zhang, Tunable three-dimensional nanostructured conductive polymer hydrogels for energy-storage applications, *ACS Appl. Mater. Inter.* 11 (4) (2019) 4258–4267, <https://doi.org/10.1021/acsami.8b19180>.
- [43] K. Wang, X. Zhang, X. Sun, Y. Ma, Conducting polymer hydrogel materials for high-performance flexible solid-state supercapacitors, *Sci. China Mater.* 59 (6) (2016) 412–420, <https://doi.org/10.1007/s40843-016-5062-3>.
- [44] P. Dou, Z. Liu, Z. Cao, J. Zheng, C. Wang, X. Xu, Rapid synthesis of hierarchical nanostructured Polyaniline hydrogel for high power density energy storage application and three-dimensional multilayers printing, *J. Mater. Sci.* 51 (9) (2016) 4274–4282, <https://doi.org/10.1007/s10853-016-9727-8>.
- [45] K. Wang, X. Zhang, C. Li, X. Sun, Q. Meng, Y. Ma, Z. Wei, Chemically crosslinked hydrogel film leads to integrated flexible supercapacitors with superior performance, *Adv. Mater.* 27 (45) (2015) 7451, <https://doi.org/10.1002/adma.201503543>.
- [46] W.W. Li, F.X. Gao, X.Q. Wang, N. Zhang, M.M. Ma, Strong and robust polyaniline-based supramolecular hydrogels for flexible supercapacitors, *Angew. Chem. Int. Ed.* 55 (32) (2016) 9196–9201, <https://doi.org/10.1002/anie.201603417>.
- [47] G. Zhang, Y. Chen, Y. Deng, C. Wang, A triblock copolymer design leads to robust hybrid hydrogels for high-performance flexible supercapacitors, *ACS Appl. Mater. Inter.* 9 (41) (2017) 36301–36310, <https://doi.org/10.1021/acsami.7b11572>.
- [48] Y. Shi, L. Pan, B. Liu, Y. Wang, Y. Cui, Z. Bao, G. Yu, Nanostructured conductive polypyrrole hydrogels as high-performance, flexible supercapacitor electrodes, *J. Mater. Chem. A* 2 (17) (2014) 6086–6091, <https://doi.org/10.1039/c4ta00484a>.
- [49] T. Dai, Z. Shi, C. Shen, J. Wang, Y. Lu, Self-strengthened conducting polymer hydrogels, *Synth. Met.* 160 (9–10) (2010) 1101–1106, <https://doi.org/10.1016/j.synthmet.2010.02.034>.
- [50] H.T. Guo, W.N. He, Y. Lu, X.T. Zhang, Self-crosslinked polyaniline hydrogel electrodes for electrochemical energy storage, *Carbon* 92 (2015) 133–141, <https://doi.org/10.1016/j.carbon.2015.03.062>.
- [51] B. Yao, H. Wang, Q. Zhou, M. Wu, M. Zhang, C. Li, G. Shi, Ultrahigh-conductivity polymer hydrogels with arbitrary structures, *Adv. Mater.* 29 (28) (2017) 1700974, <https://doi.org/10.1002/adma.201700974>.
- [52] L. Zhang, Q. Liu, J. Qiu, C. Yang, C. Wei, C. Liu, L. Lao, Design and fabrication of an all-solid-state polymer supercapacitor with highly mechanical flexibility based on polypyrrole hydrogel, *ACS Appl. Mater. Inter.* 9 (39) (2017) 33941–33947, <https://doi.org/10.1021/acsami.7b10321>.
- [53] X. Chu, H. Huang, H. Zhang, H. Zhang, B. Gu, H. Su, F. Liu, Y. Han, Z. Wang, N. Chen, C. Yan, W. Deng, W. Yang, Electrochemically building three-dimensional supramolecular polymer hydrogel for flexible solid-state micro-supercapacitors, *Electrochim. Acta* 301 (2019) 136–144, <https://doi.org/10.1016/j.electacta.2019.01.165>.
- [54] S. Iijima, Helical microtubules of graphitic carbon, *Nature* 354 (6348) (1991) 56–58, <https://doi.org/10.1038/354056a0>.
- [55] N. Rouhi, D. Jain, P.J. Burke, High-performance semiconducting nanotube inks: progress and prospects, *ACS Nano* 5 (11) (2011) 8471–8487, <https://doi.org/10.1021/nn201828y>.
- [56] Z. Yang, J. Deng, X. Chen, J. Ren, H. Peng, A highly stretchable, fiber-shaped supercapacitor, *Angew. Chem. Int. Edit.* 52 (50) (2013) 13453–13457, <https://doi.org/10.1002/anie.201307619>.
- [57] L.B. Hu, D.S. Hecht, G. Gruner, Carbon nanotube thin films: fabrication, properties, and applications, *Chem. Rev.* 110 (10) (2010) 5790–5844, <https://doi.org/10.1021/cr9002962>.
- [58] H. Fan, H. Wang, N. Zhao, X. Zhang, J. Xu, Hierarchical nanocomposite of polyaniline nanorods grown on the surface of carbon nanotubes for high-performance supercapacitor electrode, *J. Mater. Chem.* 22 (6) (2012) 2774–2780, <https://doi.org/10.1039/c1jm14311e>.
- [59] Z.B. Cai, L. Li, J. Ren, L.B. Qiu, H.J. Lin, H.S. Peng, Flexible, weavable and efficient microsupercapacitor wires based on polyaniline composite fibers incorporated with aligned carbon nanotubes, *J. Mater. Chem. A* 1 (2) (2013) 258–261, <https://doi.org/10.1039/c2ta00274d>.
- [60] C. Meng, C. Liu, S. Fan, Flexible carbon nanotube/polyaniline paper-like films and their enhanced electrochemical properties, *Electrochem. Commun.* 11 (1) (2009) 186–189, <https://doi.org/10.1016/j.elecom.2008.11.005>.

- [61] J. Zhang, L.-B. Kong, B. Wang, Y.-C. Luo, L. Kang, In-situ electrochemical polymerization of multi-walled carbon nanotube/polyaniline composite films for electrochemical supercapacitors, *Synthetic. Met.* 159 (3–4) (2009) 260–266, <https://doi.org/10.1016/j.synthmet.2008.09.018>.
- [62] X. Yan, Z. Tai, J. Chen, Q. Xue, Fabrication of carbon nanofiber-polyaniline composite flexible paper for supercapacitor, *Nanoscale* 3 (1) (2011) 212–216, <https://doi.org/10.1039/c0nr00470g>.
- [63] H. Zhang, H. Su, L. Zhang, B. Zhang, F. Chun, X. Chu, W. He, W. Yang, Flexible supercapacitors with high areal capacitance based on hierarchical carbon tubular nanostructures, *J. Power Sources* 331 (2016) 332–339, <https://doi.org/10.1016/j.jpowsour.2016.09.064>.
- [64] S. He, X. Hu, S. Chen, H. Hu, M. Hanif, H. Hou, Needle-like polyaniline nanowires on graphite nanofibers: hierarchical micro/nano-architecture for high performance supercapacitors, *J. Mater. Chem.* 22 (11) (2012) 5114, <https://doi.org/10.1039/c2jm15668g>.
- [65] Q. Wu, Y.X. Xu, Z.Y. Yao, A.R. Liu, G.Q. Shi, Supercapacitors Based on Flexible Graphene/Polyaniline Nanofiber Composite Films, *ACS Nano* 4 (4) (2010) 1963–1970, <https://doi.org/10.1021/nn1000035>.
- [66] J.J. Xu, K. Wang, S.Z. Zu, B.H. Han, Z.X. Wei, Hierarchical nanocomposites of polyaniline nanowire arrays on graphene oxidized sheets with synergistic effect for energy storage, *ACS Nano* 4 (9) (2010) 5019–5026, <https://doi.org/10.1021/nn1006539>.
- [67] Y. Zou, R. Liu, W. Zhong, W. Yang, Mechanically robust double-crosslinked network functionalized graphene/polyaniline stiff hydrogels for superior performance supercapacitors, *J. Mater. Chem. A* 6 (18) (2018) 8568–8578, <https://doi.org/10.1039/c8ta00860d>.
- [68] H.P. de Oliveira, S.A. Sydlík, T.M. Swager, Supercapacitors from Free-standing polypyrrole/graphene nanocomposites, *J. Phys. Chem. C* 117 (20) (2013) 10270–10276, <https://doi.org/10.1021/jp400344u>.
- [69] H. Fan, N. Zhao, H. Wang, J. Xu, F. Pan, 3D conductive network-based free-standing PANI-RGO-MWNTs hybrid film for high-performance flexible supercapacitor, *J. Mater. Chem. A* 2 (31) (2014) 12340–12347, <https://doi.org/10.1039/c4ta02118e>.
- [70] M. Faraji, H. Mohammadzadeh Aydisheh, Flexible free-standing polyaniline/graphene/carbon nanotube plastic films with enhanced electrochemical activity for an all-solid-state flexible supercapacitor device, *New J. Chem.* 43 (11) (2019) 4539–4546, <https://doi.org/10.1039/c9nj00043g>.
- [71] H. Zhou, H.-J. Zhai, A highly flexible solid-state supercapacitor based on the carbon nanotube doped graphene oxide/polypyrrole composites with superior electrochemical performances, *Org. Electron.* 37 (2016) 197–206, <https://doi.org/10.1016/j.orgel.2016.06.036>.
- [72] H. Zhou, X. Zhi, Ternary composite electrodes based on poly(3,4-ethylenedioxythiophene)/carbon nanotubes–carboxyl graphene for improved electrochemical capacitive performances, *Synthetic. Met.* 234 (2017) 139–144, <https://doi.org/10.1016/j.synthmet.2017.10.011>.
- [73] D. Qu, L. Wang, D. Zheng, L. Xiao, B. Deng, D. Qu, An asymmetric supercapacitor with highly dispersed nano-Bi₂O₃ and active carbon electrodes, *J. Power Sources* 269 (2014) 129–135, <https://doi.org/10.1016/j.jpowsour.2014.06.084>.
- [74] D. Pech, M. Brunet, H. Durou, P. Huang, V. Mochalin, Y. Gogotsi, P.L. Taberna, P. Simon, Ultrahigh-power micrometer-sized supercapacitors based on onion-like carbon, *Nat. Nanotechnol.* 5 (9) (2010) 651–654, <https://doi.org/10.1038/NNANO.2010.162>.
- [75] H. Zhang, L. Zhang, J. Chen, H. Su, F. Liu, W. Yang, One-step synthesis of hierarchically porous carbons for high-performance electric double layer supercapacitors, *J. Power Sources* 315 (2016) 120–126, <https://doi.org/10.1016/j.jpowsour.2016.03.005>.
- [76] Z. Zhang, Y. Zhao, S. Chen, D. Xie, X. Yao, P. Cui, X. Xu, An advanced construction strategy of all-solid-state lithium batteries with excellent interfacial compatibility and ultralong cycle life, *J. Mater. Chem. A* 5 (2017) 16984–16993, <https://doi.org/10.1039/c7ta04320a>.
- [77] D. Li, L. Chen, T. Wang, L.Z. Fan, 3D fiber-network-reinforced bicontinuous composite solid electrolyte for dendrite-free lithium metal batteries, *ACS Appl. Mater. Inter.* 10 (8) (2018) 7069–7078, <https://doi.org/10.1021/acsami.7b18123>.
- [78] J. Chmiola, C. Largeot, P.L. Taberna, P. Simon, Y. Gogotsi, Monolithic carbide-derived carbon films for micro-supercapacitors, *Science* 328 (5977) (2010) 480–483, <https://doi.org/10.1126/science.1184126>.
- [79] F. Miao, C. Shao, X. Li, K. Wang, N. Lu, Y. Liu, Freestanding hierarchically porous carbon framework decorated by polyaniline as binder-free electrodes for high performance supercapacitors, *J. Power Sources* 329 (2016) 516–524, <https://doi.org/10.1016/j.jpowsour.2016.08.111>.
- [80] M. Liu, B. Li, H. Zhou, C. Chen, Y. Liu, T. Liu, Extraordinary rate capability achieved by a 3D “skeleton/skin” carbon aerogel-polyaniline hybrid with vertically aligned pores, *Chem. Commun.* 53 (19) (2017) 2810–2813, <https://doi.org/10.1039/c7cc00121e>.
- [81] H. He, L. Ma, S. Fu, M. Gan, L. Hu, H. Zhang, F. Xie, M. Jiang, Fabrication of 3D ordered honeycomb-like nitrogen-doped carbon/PANI composite for high-performance supercapacitors, *Appl. Surf. Sci.* 484 (2019) 1288–1296, <https://doi.org/10.1016/j.apsusc.2019.04.133>.
- [82] H. Gao, K. Lian, Proton-conducting polymer electrolytes and their applications in solid supercapacitors: a review, *RSC Adv.* 4 (62) (2014) 33091–33113, <https://doi.org/10.1039/c4ra05151c>.
- [83] H. Huang, H. Su, H. Zhang, L. Xu, X. Chu, C. Hu, H. Liu, N. Chen, F. Liu, W. Deng, B. Gu, H. Zhang, W. Yang, Extraordinary areal and volumetric performance of flexible solid-state micro-supercapacitors based on highly conductive freestanding Ti₃C₂T_x films, *Adv. Electron. Mater.* 4 (8) (2018) 1800179, <https://doi.org/10.1002/aeml.201800179>.
- [84] L. Dagouset, G. Pognon, G.T.M. Nguyen, F. Vidal, S. Jus, P.-H. Aubert, Self-standing gel polymer electrolyte for improving supercapacitor thermal and electrochemical stability, *J. Power Sources* 391 (2018) 86–93, <https://doi.org/10.1016/j.jpowsour.2018.04.073>.
- [85] J. Duay, E. Gillette, R. Liu, S.B. Lee, Highly flexible pseudocapacitor based on freestanding heterogeneous MnO₂/conductive polymer nanowire arrays, *Phys. Chem. Chem. Phys.* 14 (10) (2012) 3329–3337, <https://doi.org/10.1039/c2cp00019a>.
- [86] L. Li, F. Lu, C. Wang, F. Zhang, W. Liang, S. Kuga, Z. Dong, Y. Zhao, Y. Huang, M. Wu, Flexible double-cross-linked cellulose-based hydrogel and aerogel membrane for supercapacitor separator, *J. Mater. Chem. A* 6 (47) (2018) 24468–24478, <https://doi.org/10.1039/c8ta07751g>.
- [87] N.A. Choudhury, P.W.C. Northrop, A.C. Crothers, S. Jain, V.R. Subramanian, Chitosan hydrogel-based electrode binder and electrolyte membrane for EDLCs: experimental studies and model validation, *J. Appl. Electrochem.* 42 (11) (2012) 935–943, <https://doi.org/10.1007/s10800-012-0469-2>.
- [88] Y.S. Yoon, W.I. Cho, J.H. Lim, D.J. Choi, Solid-state thin-film supercapacitor with ruthenium oxide and solid electrolyte thin films, *J. Power Sources* 101 (1) (2001) 126–129, [https://doi.org/10.1016/S0378-7753\(01\)00484-0](https://doi.org/10.1016/S0378-7753(01)00484-0).
- [89] Y. Wang, All solid-state supercapacitor with phosphotungstic acid as the proton-conducting electrolyte, *Solid State Ionics* 166 (1–2) (2004) 61–67, <https://doi.org/10.1016/j.ssi.2003.11.001>.
- [90] B.E. Francisco, C.M. Jones, S.-H. Lee, C.R. Stoldt, Nanostructured all-solid-state supercapacitor based on Li₂S-P₂S₅ glass-ceramic electrolyte, *Appl. Phys. Lett.* 100 (10) (2012) 103902, <https://doi.org/10.1063/1.3693521>.
- [91] S. Petty-Weeks, J.J. Zupancic, J.R. Swedo, Proton conducting interpenetrating polymer networks, *Solid State Ionics* 31 (1988) 117–125, [https://doi.org/10.1016/0167-2738\(88\)90295-0](https://doi.org/10.1016/0167-2738(88)90295-0).
- [92] K. Wang, W. Zou, B. Quan, A. Yu, H. Wu, P. Jiang, Z. Wei, An all-solid-state flexible micro-supercapacitor on a chip, *Adv. Energy Mater.* 1 (6) (2011) 1068–1072, <https://doi.org/10.1002/aeml.201100488>.
- [93] X. Xiao, X. Peng, H. Jin, T. Li, C. Zhang, B. Gao, B. Hu, K. Huo, J. Zhou, Freestanding mesoporous VN/CNT hybrid electrodes for flexible all-solid-state supercapacitors, *Adv. Mater.* 25 (36) (2013) 5091–5097, <https://doi.org/10.1002/adma.201301465>.
- [94] H. Gao, K. Lian, High rate all-solid electrochemical capacitors using proton conducting polymer electrolytes, *J. Power Sources* 196 (20) (2011) 8855–8857, <https://doi.org/10.1016/j.jpowsour.2011.06.032>.
- [95] H. Gao, K. Lian, Advanced proton conducting membrane for ultra-high rate solid flexible electrochemical capacitors, *J. Mater. Chem.* 22 (39) (2012) 21272–21278, <https://doi.org/10.1039/c2jm34840c>.
- [96] B. Karaman, A. Bozkurt, Enhanced performance of supercapacitor based on boric acid doped PVA-H₂SO₄ gel polymer electrolyte system, *Int. J. Hydrogen Energy* 43 (12) (2018) 6229–6237, <https://doi.org/10.1016/j.ijhydene.2018.02.032>.
- [97] O.G. Abdullah, S.B. Aziz, M.A. Rasheed, Incorporation of NH₄NO₃ into MC-PVA blend-based polymer to prepare proton-conducting polymer electrolyte films, *Ionics* 24 (3) (2017) 777–785, <https://doi.org/10.1007/s11581-017-2228-1>.
- [98] M.F. Shukur, M.F.Z. Kadir, Hydrogen ion conducting starch-chitosan blend based electrolyte for application in electrochemical devices, *Electrochim. Acta* 158 (2015) 152–165, <https://doi.org/10.1016/j.electacta.2015.01.167>.
- [99] J. Naik, R.F. Bhajantri, Physical and Electrochemical Studies on Ceria Filled PVA Proton Conducting Polymer Electrolyte for Energy Storage Applications, *J. Inorg. Organomet. Polym. Mater.* 28 (3) (2018) 906–919, <https://doi.org/10.1007/s10904-018-0801-3>.
- [100] V. Vijayakumar, M. Ghosh, A. Torris, N. Chandran, S.B. Nair, M.V. Badiger, S. Kurungot, Water-in-acid gel polymer electrolyte realized through a phosphoric acid-enriched polyelectrolyte matrix toward solid-state supercapacitors, *ACS Sustain. Chem. Eng.* 6 (10) (2018) 12630–12640, <https://doi.org/10.1021/acsschemeng.8b01175>.
- [101] F. Yu, M. Huang, J. Wu, Z. Qiu, L. Fan, J. Lin, Y. Lin, A redox-mediator-doped gel polymer electrolyte applied in quasi-solid-state supercapacitors, *J. Appl. Polym. Sci.* 131 (2) (2014) 39784, <https://doi.org/10.1002/APP.39784>.
- [102] A. Lewandowski, M. Zajder, E. Frackowiak, F. Beguin, Supercapacitor based on activated carbon and polyethylene oxide-KOH-H₂O polymer electrolyte, *Electrochim. Acta* 46 (18) (2001) 2777–2780, [https://doi.org/10.1016/S0013-4686\(01\)00496-0](https://doi.org/10.1016/S0013-4686(01)00496-0).
- [103] X. Lu, G. Wang, T. Zhai, M. Yu, S. Xie, Y. Ling, C. Liang, Y. Tong, Y. Li, Stabilized TiN nanowire arrays for high-performance and flexible supercapacitors, *Nano Lett.* 12 (10) (2012) 5376–5381, <https://doi.org/10.1021/nl302761z>.
- [104] F. Barzegar, J.K. Dangbegnon, A. Bello, D.Y. Momodu, A.T.C. Johnson, N. Manyala, Effect of conductive additives to gel electrolytes on activated carbon-based supercapacitors, *AIP Adv.* 5 (9) (2015) 97171, <https://doi.org/10.1063/1.4931956>.
- [105] N.A. Choudhury, A.K. Shukla, S. Sampath, S. Pitchumani, Cross-linked polymer hydrogel electrolytes for electrochemical capacitors, *J. Electrochem. Soc.* 153 (3) (2006) A614–A620, <https://doi.org/10.1149/1.2164810>.
- [106] N. Vassal, E. Salmon, J.F. Fauvarque, Electrochemical properties of an alkaline solid polymer electrolyte based on P(ECH-co-EO), *Electrochim. Acta* 45 (2000) 1527–1532, [https://doi.org/10.1016/S0013-4686\(99\)00369-2](https://doi.org/10.1016/S0013-4686(99)00369-2).
- [107] Z. Sun, A. Yuan, Electrochemical performance of nickel hydroxide/activated carbon supercapacitors using a modified polyvinyl alcohol based alkaline polymer electrolyte, *Chin. J. Chem. Eng.* 17 (2009) 150–155, [https://doi.org/10.1016/S1004-9541\(09\)60047-1](https://doi.org/10.1016/S1004-9541(09)60047-1).
- [108] X. Hu, L. Fan, G. Qin, Z. Shen, J. Chen, M. Wang, J. Yang, Q. Chen, Flexible and low temperature resistant double network alkaline gel polymer electrolyte with dual-role KOH for supercapacitor, *J. Power. Sources* 414 (2019) 201–209, <https://doi.org/10.1016/j.jpowsour.2019.04.073>.

- doi.org/10.1016/j.jpowsour.2019.01.006.
- [109] G. Ma, J. Li, K. Sun, H. Peng, J. Mu, Z. Lei, High performance solid-state supercapacitor with PVA-KOH-K₂[Fe(CN)₆] gel polymer as electrolyte and separator, *J. Power. Sources* 256 (2014) 281–287, <https://doi.org/10.1016/j.jpowsour.2014.01.062>.
- [110] G. Ma, E. Feng, K. Sun, H. Peng, J. Li, Z. Lei, A novel and high-effective redox-mediated gel polymer electrolyte for supercapacitor, *Electrochim. Acta* 135 (2014) 461–466, <https://doi.org/10.1016/j.electacta.2014.05.045>.
- [111] Z. Fadakar, N. Nasirizadeh, S.M. Bidoki, Z. Shekari, V. Mottaghtalab, Fabrication of a supercapacitor with a PVA-KOH-KI electrolyte and nanosilver flexible electrodes, *Microelectron. Eng.* 140 (2015) 29–32, <https://doi.org/10.1016/j.mee.2015.05.004>.
- [112] H. Yu, J. Wu, L. Fan, K. Xu, X. Zhong, Y. Lin, J. Lin, Improvement of the performance for quasi-solid-state supercapacitor by using PVA-KOH-KI polymer gel electrolyte, *Electrochim. Acta.* 56 (2011) 6881–6886, <https://doi.org/10.1016/j.electacta.2011.06.039>.
- [113] C. Liu, H. Liang, D. Wu, X. Lu, Q. Wang, Direct semiconductor laser writing of few-layer graphene polyhedra networks for flexible solid-state supercapacitor, *Adv. Electron. Mater.* 4 (2018) 1800092, <https://doi.org/10.1002/aem.201800092>.
- [114] A.M. Patil, V.C. Lokhande, U.M. Patil, P.A. Shinde, C.D. Lokhande, High performance all-solid-state asymmetric supercapacitor device based on 3D nanospheres of β-MnO₂ and nanoflowers of O-SnS, *ACS Sustainable Chem. Eng.* 6 (2017) 787–802, <https://doi.org/10.1021/acsuschemeng.7b03136>.
- [115] N. Lu, X. Zhang, R. Na, W. Ma, C. Zhang, Y. Luo, Y. Mu, S. Zhang, G. Wang, High performance electrospun Li⁺-functionalized sulfonated poly(ether ether ketone)/PVA based nanocomposite gel polymer electrolyte for solid-state electric double layer capacitors, *J. Colloid Interface Sci.* 534 (2019) 672–682, <https://doi.org/10.1016/j.jcis.2018.09.027>.
- [116] G. Lee, J.W. Kim, H. Park, J.Y. Lee, H. Lee, C. Song, S.W. Jin, K. Keum, C.H. Lee, J.S. Ha, Skin-like, dynamically stretchable, planar supercapacitors with buckled carbon nanotube/Mn-Mo mixed oxide electrodes and air-stable organic electrolyte, *ACS Nano* 13 (1) (2018) 855–866, <https://doi.org/10.1021/acsnano.8b08645>.
- [117] A. Virya, K. Lian, Lithium polyacrylate-polyacrylamide blend as polymer electrolytes for solid-state electrochemical capacitors, *Electrochem. Commun.* 97 (2018) 77–81, <https://doi.org/10.1016/j.elecom.2018.10.026>.
- [118] J. Tang, P. Yuan, C. Cai, Y. Fu, X. Ma, Combining nature-inspired, graphene-wrapped flexible electrodes with nanocomposite polymer electrolyte for asymmetric capacitive energy storage, *Adv. Energy Mater.* 6 (2016) 1600813, <https://doi.org/10.1002/aem.201600813>.
- [119] X. Yang, F. Zhang, L. Zhang, T. Zhang, Y. Huang, Y. Chen, A high-performance graphene oxide-doped ion gel as gel polymer electrolyte for all-solid-state supercapacitor applications, *Adv. Funct. Mater.* 23 (2013) 3353–3360, <https://doi.org/10.1002/adfm.201203556>.
- [120] Q.-M. Tu, L.-Q. Fan, F. Pan, J.-L. Huang, Y. Gu, J.-M. Lin, M.-L. Huang, Y.-F. Huang, J.-H. Wu, Design of a novel redox-active gel polymer electrolyte with a dual-role ionic liquid for flexible supercapacitors, *Electrochim. Acta* 268 (2018) 562–568, <https://doi.org/10.1016/j.electacta.2018.02.008>.
- [121] S.-W. Baek, J.-M. Lee, T.Y. Kim, M.-S. Song, Y. Park, Garnet related lithium ion conductor processed by spark plasma sintering for all solid state batteries, *J. Power Sources* 249 (2014) 197–206, <https://doi.org/10.1016/j.jpowsour.2013.10.089>.
- [122] F. Han, T. Gao, Y. Zhu, K.J. Gaskell, C. Wang, A battery made from a single material, *Adv. Mater.* 27 (2015) 3473–3483, <https://doi.org/10.1002/adma.201500180>.
- [123] B. Liu, P. Soares, C. Checkles, Y. Zhao, G. Yu, Three-dimensional hierarchical ternary nanostructures for high-performance Li-ion battery anodes, *Nano Lett.* 13 (2013) 3414–3419, <https://doi.org/10.1021/nl401880v>.
- [124] Y. Shi, J. Zhang, A.M. Bruck, Y. Zhang, J. Li, E.A. Stach, K.J. Takeuchi, A.C. Marschilok, E.S. Takeuchi, G. Yu, A tunable 3D nanostructured conductive gel framework electrode for high-performance lithium ion batteries, *Adv. Mater.* 29 (22) (2017) 1603922, <https://doi.org/10.1002/adma.201603922>.
- [125] Y. Shi, X. Zhou, J. Zhang, A.M. Bruck, A.C. Bond, A.C. Marschilok, K.J. Takeuchi, E.S. Takeuchi, G. Yu, Nanostructured conductive polymer gels as a general framework material to improve electrochemical performance of cathode materials in Li-ion batteries, *Nano Lett.* 17 (2017) 1906–1914, <https://doi.org/10.1021/acs.nanolett.6b05227>.
- [126] M.B. McDonald, P.T. Hammond, Efficient transport networks in a dual electron/lithium-conducting polymeric composite for electrochemical applications, *ACS Appl. Mater. Inter.* 10 (2018) 15681–15690, <https://doi.org/10.1021/acsmi.8b01519>.
- [127] N. Li, Z. Chen, W. Ren, F. Li, H.M. Cheng, Flexible graphene-based lithium ion batteries with ultrafast charge and discharge rates, *Proc. Natl. Acad. Sci. U.S.A.* 109 (2012) 17360–17365, <https://doi.org/10.1073/pnas.1210072109>.
- [128] J. Xu, M. Wang, N.P. Wickramaratne, M. Jaroniec, S. Dou, L. Dai, High-performance sodium ion batteries based on a 3D anode from nitrogen-doped graphene foams, *Adv. Mater.* 27 (2015) 2042–2048, <https://doi.org/10.1002/adma.201405370>.
- [129] Y. Zhang, Y. Huang, G. Yang, F. Bu, K. Li, I. Shakir, Y. Xu, Dispersion-assembly approach to synthesize three-dimensional graphene/polymer composite aerogel as a powerful organic cathode for rechargeable Li and Na batteries, *ACS Appl. Mater. Inter.* 9 (2017) 15549–15556, <https://doi.org/10.1021/acsmi.7b03687>.
- [130] M.T. Jeena, T. Bok, S.H. Kim, S. Park, J.-Y. Kim, S. Park, J.-H. Ryu, A siloxane-incorporated copolymer as an in situ cross-linkable binder for high performance silicon anodes in Li-ion batteries, *Nanoscale* 8 (2016) 9245–9253, <https://doi.org/10.1039/c6nr01559j>.
- [131] L. Fan, H.L. Zhuang, W. Zhang, Y. Fu, Z. Liao, Y. Lu, Stable lithium electrodeposition at ultra-high current densities enabled by 3D PMF/Li composite anode, *Adv. Energy Mater.* 8 (15) (2018) 1703360, <https://doi.org/10.1002/aem.201703360>.
- [132] Y. Guo, Y. Ouyang, D. Li, Y. Wei, T. Zhai, H. Li, PMMA-assisted Li deposition towards 3D continuous dendrite-free lithium anode, *Energy Storage Mater.* 16 (2019) 203–211, <https://doi.org/10.1016/j.ensm.2018.05.012>.
- [133] H.H. Wei, Q. Zhang, Y. Wang, Y.J. Li, J.C. Fan, Q.J. Xu, Y.L. Min, Baby diaper-inspired construction of 3D porous composites for long-term lithium-ion batteries, *Adv. Funct. Mater.* 28 (3) (2018) 1704440, <https://doi.org/10.1002/adfm.201704440>.
- [134] C. O'Meara, M.P. Karushev, I.A. Polozhentceva, S. Dharmasena, H. Cho, B.J. Yurkovich, S. Kogan, J.H. Kim, Nickel-Salen-type polymer as conducting agent and binder for carbon-free cathodes in lithium-ion batteries, *ACS Appl. Mater. Inter.* 11 (2019) 525–533, <https://doi.org/10.1021/acsmi.8b13742>.
- [135] K. Hatakeyama-Sato, H. Wakamatsu, R. Katagiri, K. Oyaizu, H. Nishide, An Ultrahigh output rechargeable electrode of a hydrophilic radical polymer/nanocarbon hybrid with an exceptionally large current density beyond 1 A cm⁻², *Adv. Mater.* 30 (2018) e1800900, <https://doi.org/10.1002/adma.201800900>.
- [136] T. Liu, Q. Chu, C. Yan, S. Zhang, Z. Lin, J. Lu, Interweaving 3D network binder for high-areal-capacity Si anode through combined hard and soft polymers, *Adv. Energy Mater.* 9 (3) (2019) 1802645, <https://doi.org/10.1002/aem.201802645>.
- [137] B. Xu, H. Zhai, X. Liao, B. Qie, J. Mandal, T. Gong, L. Tan, X. Yang, K. Sun, Q. Cheng, M. Chen, Y. Miao, M. Wei, B. Zhu, Y. Fu, A. Li, X. Chen, W. Min, C.-W. Nan, Y.-H. Lin, Y. Yang, Porous insulating matrix for lithium metal anode with long cycling stability and high power, *Energy Storage Mater.* 17 (2019) 31–37, <https://doi.org/10.1016/j.ensm.2018.11.035>.
- [138] C. Zhang, S. Liu, G. Li, C. Zhang, X. Liu, J. Luo, Incorporating ionic paths into 3D conducting scaffolds for high volumetric and areal capacity, high rate lithium-metal anodes, *Adv. Mater.* (2018) e1801328, <https://doi.org/10.1002/adma.201801328>.
- [139] Z. Wang, M. Li, C. Ruan, C. Liu, C. Zhang, C. Xu, K. Edström, M. Strømme, L. Nyholm, Conducting polymer paper-derived mesoporous 3D N-doped carbon current collectors for Na and Li metal anodes: a combined experimental and theoretical study, *J. Phys. Chem. C* 122 (2018) 23352–23363, <https://doi.org/10.1021/acs.jpcc.8b07481>.
- [140] Y. Gong, K. Fu, S. Xu, J. Dai, T.R. Hamann, L. Zhang, G.T. Hitz, Z. Fu, Z. Ma, D.W. McOwen, X. Han, L. Hu, E.D. Wachsmann, Lithium-ion conductive ceramic textile: a new architecture for flexible solid-state lithium metal batteries, *Mater. Today* 21 (2018) 594–601, <https://doi.org/10.1016/j.mattod.2018.01.001>.
- [141] P. Zhu, C. Yan, J. Zhu, J. Zang, Y. Li, H. Jia, X. Dong, Z. Du, C. Zhang, N. Wu, M. Dirican, X. Zhang, Flexible electrolyte-cathode bilayer framework with stabilized interface for room-temperature all-solid-state lithium-sulfur batteries, *Energy Storage Mater.* 17 (2019) 220–225, <https://doi.org/10.1016/j.ensm.2018.11.009>.
- [142] S. Qi, X. Zhang, W. Lv, Y. Zhang, D. Kong, Z. Huang, Q.H. Yang, Electrode design from “internal” to “external” for high stability silicon anodes in lithium-ion batteries, *ACS Appl. Mater. Inter.* 11 (15) (2019) 14142–14149, <https://doi.org/10.1021/acsmi.9b02206>.
- [143] H. Zhang, X. Hu, Y. Zhang, S. Wang, F. Xin, X. Chen, D. Yu, 3D-crosslinked tannic acid/poly(ethylene oxide) complex as a three-in-one multifunctional binder for high-sulfur-loading and high-stability cathodes in lithium-sulfur batteries, *Energy Storage Mater.* 17 (2019) 293–299, <https://doi.org/10.1016/j.ensm.2018.07.006>.
- [144] A.I. Pitillas Martinez, F. Aguesse, L. Otaegui, M. Schneider, A. Roters, A. Llordés, L. Buannic, The cathode composition, a key player in the success of Li-metal solid-state batteries, *J. Phys. Chem. C* 123 (2019) 3270–3278, <https://doi.org/10.1021/acs.jpcc.8b04626>.
- [145] D.H. Kim, M.Y. Kim, S.H. Yang, H.M. Ryu, H.Y. Jung, H.-J. Ban, S.-J. Park, J.S. Lim, H.-S. Kim, Fabrication and electrochemical characteristics of NCM-based all-solid lithium batteries using nano-grade garnet Al-LLZO powder, *J. Ind. Eng. Chem.* 71 (2019) 445–451, <https://doi.org/10.1016/j.jiec.2018.12.001>.
- [146] Z.P. Wan, D.N. Lei, W. Yang, C. Liu, K. Shi, X.G. Hao, L. Shen, W. Lv, B.H. Li, Q.H. Yang, F.Y. Kang, Y.B. He, Low resistance-integrated all-solid-state battery achieved by Li₇La₃Zr₂O₁₂ nanowire upgrading polyethylene oxide (PEO) composite electrolyte and PEO cathode binder, *Adv. Funct. Mater.* 29 (1) (2019) 1805301, <https://doi.org/10.1002/adfm.201805301>.
- [147] R. Oriňáková, A. Fedorková, A. Oriňák, Effect of PPy/PEG conducting polymer film on electrochemical performance of LiFePO₄ cathode material for Li-ion batteries, *Chem. Pap.* 67 (8) (2013) 860–875, <https://doi.org/10.2478/s11696-013-0350-8>.
- [148] M.E. Bhosale, K. Krishnamoorthy, Chemically reduced organic small-molecule-based lithium battery with improved efficiency, *Chem. Mater.* 27 (2015) 2121–2126, <https://doi.org/10.1021/cm5046786>.
- [149] T.B. Schon, B.T. McAllister, P.F. Li, D.S. Seferos, The rise of organic electrode materials for energy storage, *Chem. Soc. Rev.* 45 (2016) 6345–6404, <https://doi.org/10.1039/c6cs00173d>.
- [150] Z. Song, H. Zhou, Towards sustainable and versatile energy storage devices: an overview of organic electrode materials, *Energy Environ. Sci.* 6 (8) (2013) 2280–2301, <https://doi.org/10.1039/c3ee40709h>.
- [151] C. Luo, Y. Zhu, Y. Xu, Y. Liu, T. Gao, J. Wang, C. Wang, Graphene oxide wrapped croconic acid disodium salt for sodium ion battery electrodes, *J. Power Sources* 250 (2014) 372–378, <https://doi.org/10.1016/j.jpowsour.2013.10.131>.
- [152] Z. Song, Y. Qian, X. Liu, T. Zhang, Y. Zhu, H. Yu, M. Otani, H. Zhou, A quinone-based oligomeric lithium salt for superior Li-organic batteries, *Energy Environ. Sci.* 7 (2014) 4077–4086, <https://doi.org/10.1039/c4ee02575j>.
- [153] X. Shen, H. Liu, X.-B. Cheng, C. Yan, J.-Q. Huang, Beyond lithium ion batteries: higher energy density battery systems based on lithium metal anodes, *Energy*

- Storage Mater. 12 (2018) 161–175, <https://doi.org/10.1016/j.ensm.2017.12.002>.
- [154] R. Schmuch, R. Wagner, G. Hörpel, T. Placke, M. Winter, Performance and cost of materials for lithium-based rechargeable automotive batteries, *Nat. Energy* 3 (2018) 267–278, <https://doi.org/10.1038/s41560-018-0107-2>.
- [155] V. Aravindan, Y.-S. Lee, S. Madhavi, Research progress on negative electrodes for practical Li-ion batteries: beyond carbonaceous anodes, *Adv. Energy Mater.* 5 (13) (2015) 1402225, <https://doi.org/10.1002/aenm.201402225>.
- [156] W. Xu, J. Wang, F. Ding, X. Chen, E. Nasybulin, Y. Zhang, J.-G. Zhang, Lithium metal anodes for rechargeable batteries, *Energy Environ. Sci.* 7 (2014) 513–537, <https://doi.org/10.1039/C3EE40795K>.
- [157] H. Ye, Y.-X. Yin, S.-F. Zhang, Y. Shi, L. Liu, X.-X. Zeng, R. Wen, Y.-G. Guo, L.-J. Wan, Synergism of Al-containing solid electrolyte interphase layer and Al-based colloidal particles for stable lithium anode, *Nano Energy* 36 (2017) 411–417, <https://doi.org/10.1016/j.nanoen.2017.04.056>.
- [158] N.W. Li, Y.X. Yin, C.P. Yang, Y.G. Guo, An artificial solid electrolyte interphase layer for stable lithium metal anodes, *Adv. Mater.* 28 (2016) 1853–1858, <https://doi.org/10.1002/adma.201504526>.
- [159] X.B. Cheng, R. Zhang, C.Z. Zhao, F. Wei, J.G. Zhang, Q. Zhang, A review of solid electrolyte interphases on lithium metal anode, *Adv. Sci.* 3 (2016) 1500213, <https://doi.org/10.1002/adv.201500213>.
- [160] Z. Liang, D. Lin, J. Zhao, Z. Lu, Y. Liu, C. Liu, Y. Lu, H. Wang, K. Yan, X. Tao, Y. Cui, Composite lithium metal anode by melt infusion of lithium into a 3D conducting scaffold with lithiophilic coating, *Proc. Natl. Acad. Sci. U.S.A* 113 (2016) 2862–2867, <https://doi.org/10.1073/pnas.1518188113>.
- [161] R. Mogi, M. Inaba, S.-K. Jeong, Y. Iriyama, T. Abe, Z. Ogumi, Effects of some organic additives on lithium deposition in propylene carbonate, *J. Electrochem. Soc.* 149 (12) (2002) A1578–A1583, <https://doi.org/10.1149/1.1516770>.
- [162] Z.-I. Takehara, Future prospects of the lithium metal anode, *J. Power Sources* 68 (1997) 82–86, [https://doi.org/10.1016/S0378-7753\(96\)02546-3](https://doi.org/10.1016/S0378-7753(96)02546-3).
- [163] D. Aurbach, E. Pollak, R. Elazari, G. Salitra, C.S. Kelley, J. Affinito, On the surface chemical aspects of very high energy density, rechargeable Li–sulfur batteries, *J. Electrochem. Soc.* 156 (8) (2009) A694–A702, <https://doi.org/10.1149/1.3148721>.
- [164] Y. Lu, Z. Tu, L.A. Archer, Stable lithium electrodeposition in liquid and nanoporous solid electrolytes, *Nat. Mater.* 13 (2014) 961–969, <https://doi.org/10.1038/NMAT4041>.
- [165] W. Li, H. Yao, K. Yan, G. Zheng, Z. Liang, Y.M. Chiang, Y. Cui, The synergistic effect of lithium polysulfide and lithium nitrate to prevent lithium dendrite growth, *Nat. Commun.* 6 (2015) 7436, <https://doi.org/10.1038/ncomms8436>.
- [166] Y. Zhang, J. Qian, W. Xu, S.M. Russell, X. Chen, E. Nasybulin, P. Bhattacharya, M.H. Engelhard, D. Mei, R. Cao, F. Ding, A.V. Cresce, K. Xu, J.G. Zhang, Dendrite-free lithium deposition with self-aligned nanorod structure, *Nano Lett.* 14 (2014) 6889–6896, <https://doi.org/10.1021/nl5039117>.
- [167] Z. Peng, N. Zhao, Z. Zhang, H. Wan, H. Lin, M. Liu, C. Shen, H. He, X. Guo, J.-G. Zhang, D. Wang, Stabilizing Li/electrolyte interface with a transplantable protective layer based on nanoscale LiF domains, *Nano Energy* 39 (2017) 662–672, <https://doi.org/10.1016/j.nanoen.2017.07.052>.
- [168] G. Zheng, S.W. Lee, Z. Liang, H.W. Lee, K. Yan, H. Yao, H. Wang, W. Li, S. Chu, Y. Cui, Interconnected hollow carbon nanospheres for stable lithium metal anodes, *Nat. Nanotechnol.* 9 (2014) 618–623, <https://doi.org/10.1038/NNANO.2014.152>.
- [169] B. Li, D. Zhang, Y. Liu, Y. Yu, S. Li, S. Yang, Flexible Ti₃C₂ MXene-lithium film with lamellar structure for ultrastable metallic lithium anodes, *Nano Energy* 39 (2017) 654–661, <https://doi.org/10.1016/j.nanoen.2017.07.023>.
- [170] H. Gao, F. Yang, Y. Zheng, Q. Zhang, J. Hao, S. Zhang, H. Zheng, J. Chen, H. Liu, Z. Guo, Three-dimensional porous cobalt phosphide nanocubes encapsulated in a graphene aerogel as an advanced anode with high coulombic efficiency for high-energy lithium-ion batteries, *ACS Appl. Mater. Inter.* 11 (2019) 5373–5379, <https://doi.org/10.1021/acami.8b19613>.
- [171] R. Ding, J. Zhang, J. Zhang, Z. Li, C. Wang, M. Chen, Core-shell Fe₂N@amorphous carbon nanocomposite-filled 3D graphene framework: an additive-free anode material for lithium-ion batteries, *Chem. Eng. J.* 360 (2019) 1063–1070, <https://doi.org/10.1016/j.cej.2018.10.177>.
- [172] J. Yu, H. Huang, Y. Gan, Y. Xia, C. Liang, J. Zhang, X. Tao, W. Zhang, A new strategy for the construction of 3D TiO₂ nanowires/reduced graphene oxide for high-performance lithium/sodium batteries, *J. Mater. Chem. A* 6 (2018) 24256–24266, <https://doi.org/10.1039/c8ta08214f>.
- [173] Z. Chen, J. Chen, F. Bu, P.O. Agboola, I. Shakir, Y. Xu, Double-hole-heterostructure frameworks enable fast, stable, and simultaneous ultrahigh gravimetric, areal, and volumetric lithium storage, *ACS Nano* 12 (2018) 12879–12887, <https://doi.org/10.1021/acsnano.8b08071>.
- [174] X. Zhang, A. Wang, R. Lv, J. Luo, A corrosion-resistant current collector for lithium metal anodes, *Energy Storage Mater.* 18 (2019) 199–204, <https://doi.org/10.1016/j.ensm.2018.09.017>.
- [175] G. Hou, Q. Sun, Q. Ai, X. Ren, X. Xu, H. Guo, S. Guo, L. Zhang, J. Feng, F. Ding, P.M. Ajayan, P. Si, L. Ci, Growth direction control of lithium dendrites in a heterogeneous lithiophilic host for ultra-safe lithium metal batteries, *J. Power Sources* 416 (2019) 141–147, <https://doi.org/10.1016/j.jpowsour.2019.01.074>.
- [176] L. Lu, J.T.M. De Hosson, Y. Pei, Three-dimensional micron-porous graphene foams for lightweight current collectors of lithium-sulfur batteries, *Carbon* 144 (2019) 713–723, <https://doi.org/10.1016/j.carbon.2018.12.103>.
- [177] S. Yuan, J.L. Bao, C. Li, Y. Xia, D.G. Truhlar, Y. Wang, Dual lithiophilic structure for uniform Li deposition, *ACS Appl. Mater. Inter.* 11 (2019) 10616–10623, <https://doi.org/10.1021/acami.8b19654>.
- [178] L.L. Lu, J. Ge, J.N. Yang, S.M. Chen, H.B. Yao, F. Zhou, S.H. Yu, Free-standing copper nanowire network current collector for improving lithium anode performance, *Nano Lett.* 16 (2016) 4431–4437, <https://doi.org/10.1021/acs.nanolett.6b01581>.
- [179] Z. Liang, G. Zheng, C. Liu, N. Liu, W. Li, K. Yan, H. Yao, P.C. Hsu, S. Chu, Y. Cui, Polymer nanofiber-guided uniform lithium deposition for battery electrodes, *Nano Lett.* 15 (2015) 2910–2916, <https://doi.org/10.1021/nl5046318>.
- [180] J.W. Choi, D. Aurbach, Promise and reality of post-lithium-ion batteries with high energy densities, *Nat. Rev. Mater.* 1 (4) (2016) 1603, <https://doi.org/10.1038/natrevmats.2016.13>.
- [181] X. Zuo, J. Zhu, P. Müller-Buschbaum, Y.-J. Cheng, Silicon based lithium-ion battery anodes: a chronicle perspective review, *Nano Energy* 31 (2017) 113–143, <https://doi.org/10.1016/j.nanoen.2016.11.013>.
- [182] H. Wu, G. Yu, L. Pan, N. Liu, M.T. McDowell, Z. Bao, Y. Cui, Stable Li-ion battery anodes by in-situ polymerization of conducting hydrogel to conformally coat silicon nanoparticles, *Nat. Commun.* 4 (2013) 1943, <https://doi.org/10.1038/ncomms2941>.
- [183] G. Xu, B. Ding, J. Pan, P. Nie, L. Shen, X. Zhang, High performance lithium–sulfur batteries: advances and challenges, *J. Mater. Chem. A* 2 (2014) 12662–12676, <https://doi.org/10.1039/c4ta02097a>.
- [184] X. Yu, H. Yang, H. Meng, Y. Sun, J. Zheng, D. Ma, X. Xu, Three-dimensional conductive gel network as an effective binder for high-performance Si electrodes in lithium-ion batteries, *ACS Appl. Mater. Inter.* 7 (2015) 15961–15967, <https://doi.org/10.1021/acami.5b04058>.
- [185] D.X. Yan, H. Pang, B. Li, R. Vajtai, L. Xu, P.G. Ren, J.H. Wang, Z.M. Li, Structured reduced graphene oxide/polymer composites for ultra-efficient electromagnetic interference shielding, *Adv. Funct. Mater.* 25 (2015) 559–566, <https://doi.org/10.1002/adfm.201403809>.
- [186] J.H. Ryu, J.W. Kim, Y.-E. Sung, S.M. Oh, Failure modes of silicon powder negative electrode in lithium secondary batteries, *Electrochem. Solid-State Lett.* 7 (10) (2004) A306–A309, <https://doi.org/10.1149/1.1792242>.
- [187] Y. Fang, R. Zhang, B. Duan, M. Liu, A. Lu, L. Zhang, Recyclable universal solvents for chitin to chitosan with various degrees of acetylation and construction of robust hydrogels, *ACS Sustainable Chem. Eng.* 5 (2017) 2725–2733, <https://doi.org/10.1021/acssuschemeng.6b03055>.
- [188] Y. Li, W. Zhou, X. Chen, X. Lu, Z. Cui, S. Xin, L. Xue, Q. Jia, J.B. Goodenough, Mastering the interface for advanced all-solid-state lithium rechargeable batteries, *Proc. Natl. Acad. Sci. U.S.A* 113 (2016) 13313–13317, <https://doi.org/10.1073/pnas.1615912113>.
- [189] Q. Wang, W.-L. Song, L.-Z. Fan, Q. Shi, Effect of alumina on triethylene glycol diacetate-2-propenoic acid butyl ester composite polymer electrolytes for flexible lithium ion batteries, *J. Power Sources* 279 (2015) 405–412, <https://doi.org/10.1016/j.jpowsour.2015.01.035>.
- [190] D. Lin, W. Liu, Y. Liu, H.R. Lee, P.C. Hsu, K. Liu, Y. Cui, High ionic conductivity of composite solid polymer electrolyte via in situ synthesis of monodispersed SiO₂ nanospheres in poly(ethylene oxide), *Nano Lett.* 16 (2016) 459–465, <https://doi.org/10.1021/acs.nanolett.5b04117>.
- [191] X. Wang, Y. Zhang, X. Zhang, T. Liu, Y.H. Lin, L. Li, Y. Shen, C.W. Nan, Lithium-salt-rich PEO/Li_{0.33}La_{0.557}TiO₃ interpenetrating composite electrolyte with three-dimensional ceramic nano-backbone for all-solid-state lithium-ion batteries, *ACS Appl. Mater. Inter.* 10 (2018) 24791–24798, <https://doi.org/10.1021/acami.8b06658>.
- [192] K.K. Fu, Y. Gong, J. Dai, A. Gong, X. Han, Y. Yao, C. Wang, Y. Wang, Y. Chen, C. Yan, Y. Li, E.D. Wachsman, L. Hu, Flexible, solid-state, ion-conducting membrane with 3D garnet nanofiber networks for lithium batteries, *Proc. Natl. Acad. Sci. U.S.A* 113 (2016) 7094–7099, <https://doi.org/10.1073/pnas.1600422113>.
- [193] W. Liu, S.W. Lee, D. Lin, F. Shi, S. Wang, A.D. Sendek, Y. Cui, Enhancing ionic conductivity in composite polymer electrolytes with well-aligned ceramic nanowires, *Nat. Energy* 2 (5) (2017) 17035, <https://doi.org/10.1038/nenergy.2017.35>.
- [194] P. Zhu, C. Yan, M. Dirican, J. Zhu, J. Zang, R.K. Selvan, C.-C. Chung, H. Jia, Y. Li, Y. Kiyak, N. Wu, X. Zhang, Li_{0.33}La_{0.557}TiO₃ ceramic nanofiber-enhanced polyethylene oxide-based composite polymer electrolytes for all-solid-state lithium batteries, *J. Mater. Chem. A* 6 (2018) 4279–4285, <https://doi.org/10.1039/c7ta10517g>.
- [195] G. Fu, T. Kyu, Effect of side-chain branching on enhancement of ionic conductivity and capacity retention of a solid copolymer electrolyte membrane, *Langmuir* 33 (2017) 13973–13981, <https://doi.org/10.1021/acs.langmuir.7b03449>.
- [196] J. Zheng, M.H. Engelhard, D. Mei, S. Jiao, B.J. Polzin, J.-G. Zhang, W. Xu, Electrolyte additive enabled fast charging and stable cycling lithium metal batteries, *Nat. Energy* 2 (3) (2017) 17012, <https://doi.org/10.1038/nenergy.2017.12>.
- [197] X.B. Cheng, T.Z. Hou, R. Zhang, H.J. Peng, C.Z. Zhao, J.Q. Huang, Q. Zhang, Dendrite-free lithium deposition induced by uniformly distributed lithium ions for efficient lithium metal batteries, *Adv. Mater.* 28 (2016) 2888–2895, <https://doi.org/10.1002/adma.201506124>.
- [198] Q. Lu, Y.B. He, Q. Yu, B. Li, Y.V. Kaneti, Y. Yao, F. Kang, Q.H. Yang, Dendrite-free, high-rate, long-life lithium metal batteries with a 3D cross-linked network polymer electrolyte, *Adv. Mater.* 29 (13) (2017) 1604460, <https://doi.org/10.1002/adma.201604460>.
- [199] J. Bentley, G.P.A. Turner, *Introduction to Paint Chemistry and Principles of Paint Technology*, CRC Press, Boca Raton, 1997.
- [200] B. Ellis, *Introduction to the Chemistry, Synthesis, Manufacture and Characterization of Epoxy Resins, Chemistry and Technology of Epoxy Resins*, Springer, Berlin, 1993, pp. 1–36.
- [201] H. Zhai, P. Xu, M. Ning, Q. Cheng, J. Mandal, Y. Yang, A flexible solid composite electrolyte with vertically aligned and connected ion-conducting nanoparticles for lithium batteries, *Nano Lett.* 17 (2017) 3182–3187, <https://doi.org/10.1021/acs.nanolett.6b01581>.

- nanolett.7b00715.
- [202] W. Wang, E. Yi, A.J. Fici, R.M. Laine, J. Kieffer, Lithium ion conducting poly(ethylene oxide)-based solid electrolytes containing active or passive ceramic nanoparticles, *J. Phys. Chem. C* 121 (2017) 2563–2573, <https://doi.org/10.1021/acs.jpcc.6b11136>.
- [203] T. Yang, J. Zheng, Q. Cheng, Y.Y. Hu, C.K. Chan, Composite polymer electrolytes with $\text{Li}_7\text{La}_3\text{Zr}_2\text{O}_{12}$ garnet-type nanowires as ceramic fillers: mechanism of conductivity enhancement and role of doping and morphology, *ACS Appl. Mater. Inter.* 9 (2017) 21773–21780, <https://doi.org/10.1021/acsami.7b03806>.
- [204] K.-S. Ji, H.-S. Moon, J.-W. Kim, J.-W. Park, Role of functional nano-sized inorganic fillers in poly(ethylene) oxide-based polymer electrolytes, *J. Power Sources* 117 (2003) 124–130, [https://doi.org/10.1016/S0378-7753\(03\)00159-9](https://doi.org/10.1016/S0378-7753(03)00159-9).
- [205] M. Keller, G.B. Appetecchi, G.-T. Kim, V. Sharova, M. Schneider, J. Schuhmacher, A. Roters, S. Passerini, Electrochemical performance of a solvent-free hybrid ceramic-polymer electrolyte based on $\text{Li}_7\text{La}_3\text{Zr}_2\text{O}_{12}$ in $\text{P}(\text{EO})_{15}$ LiTFSI, *J. Power Sources* 353 (2017) 287–297, <https://doi.org/10.1016/j.jpowsour.2017.04.014>.
- [206] C.Z. Zhao, X.Q. Zhang, X.B. Cheng, R. Zhang, R. Xu, P.Y. Chen, H.J. Peng, J.Q. Huang, Q. Zhang, An anion-immobilized composite electrolyte for dendrite-free lithium metal anodes, *Proc. Natl. Acad. Sci. U.S.A.* 114 (2017) 11069–11074, <https://doi.org/10.1073/pnas.1708489114>.
- [207] X. Fu, D. Yu, J. Zhou, S. Li, X. Gao, Y. Han, P. Qi, X. Feng, B. Wang, Inorganic and organic hybrid solid electrolytes for lithium-ion batteries, *CrystEngComm* 18 (2016) 4236–4258, <https://doi.org/10.1039/c6ce00171h>.
- [208] L. Yan, D. Han, M. Xiao, S. Ren, Y. Li, S. Wang, Y. Meng, Instantaneous carbonization of an acetylenic polymer into highly conductive graphene-like carbon and its application in lithium–sulfur batteries, *J. Mater. Chem. A* 5 (2017) 7015–7025, <https://doi.org/10.1039/c7ta01400g>.
- [209] C.H.J. Kim, C.V. Varanasi, J. Liu, Synergy of polypyrrole and carbon x-aerogel in lithium-oxygen batteries, *Nanoscale* 10 (2018) 3753–3758, <https://doi.org/10.1039/c7nr08494c>.
- [210] C.R. Matos-Perez, J.D. White, J.J. Wilker, Polymer composition and substrate influences on the adhesive bonding of a biomimetic, cross-linking polymer, *J. Am. Chem. Soc.* 134 (2012) 9498–9505, <https://doi.org/10.1021/ja303369p>.